Belgian contribution to the Physical and Biogeochemical investigations of sea ice and underlying sea water during the NB Palmer SIMBA cruise (October 2007)

by Tison, J.-L, Delille, B., de Jong, J., Vancopenolle, M., Dumont, I., Masson, F.,Brabant, F., Geilfus, N.X. and Carnat, G.

Context, Objectives and Global achievements

Our contribution to the NB Palmer SIMBA cruise has been initiated under the auspices of the IPY project “Antarctic Sea Ice in IPY” led by Dr. S. Ackley. Belgium has indeed submitted a specific IPY project entitled BASICS (Biogeochemistry of Antarctic Sea Ice and the Climate System) that has been officially endorsed, both at the national and international level, and affiliated to two main IPY projects: “ICED” (**I**ntegrated analyses of circumpolar **C**limate interactions and **E**cosystem **D**ynamics in the Southern Ocean) and “Antarctic sea ice in IPY”. The main objective of the BASICS project is **to better understand and budget exchanges of energy and matters across the ocean-sea ice- atmosphere interfaces, and to quantify their potential impact on fluxes of climatically significant gases and carbon export to the deep ocean with focus on the main biogeochemical cycles (incl. Fe) in sea ice covered oceans**.
SIBCLIM gave us an ideal opportunity to join a sea ice physics focused cruise offering the possibility to complete sea ice biogeochemical process studies during a period of about one month in an area (the Bellingshausen Sea) and at a period in time (end of winter-spring)

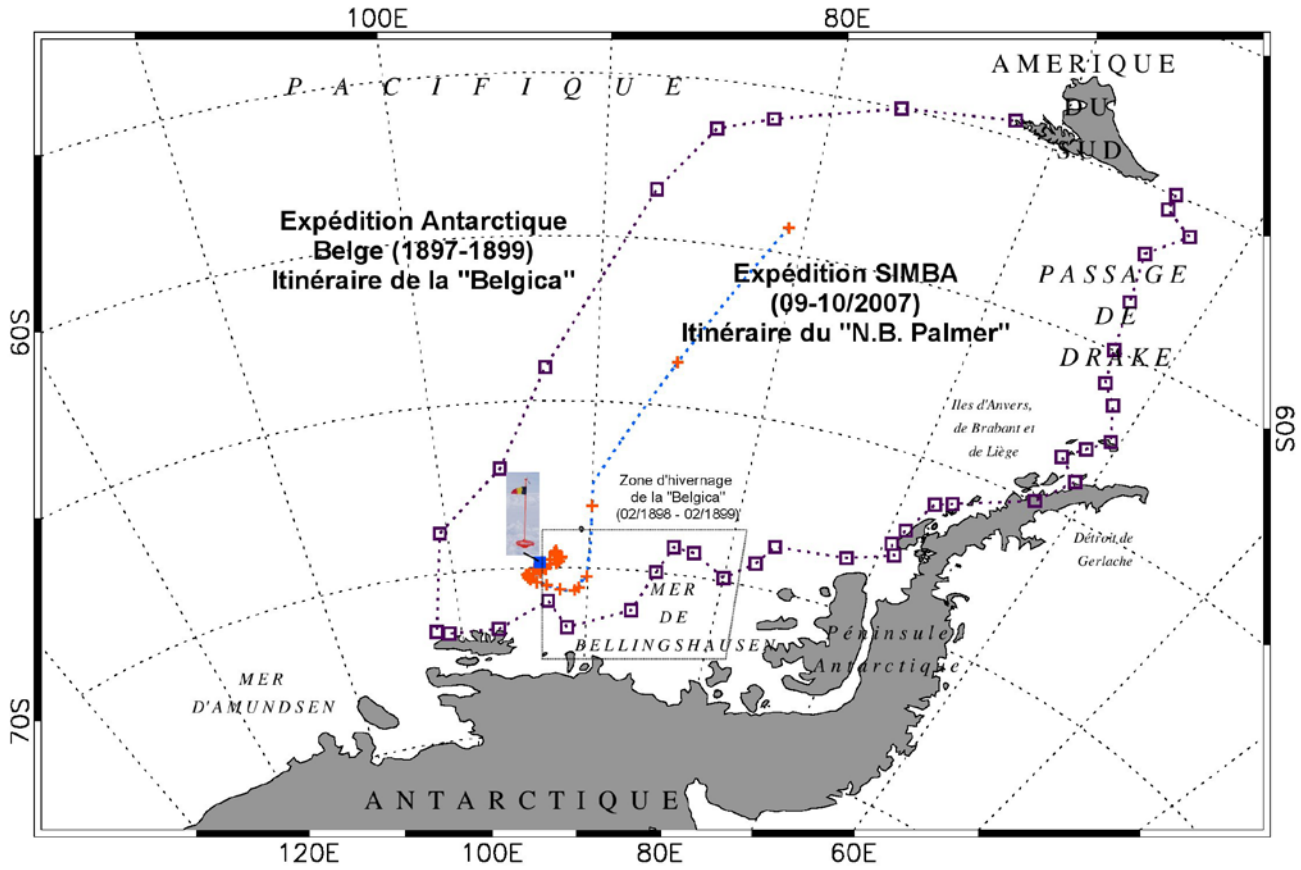

Figure 1 : The ship track of the NB Palmer SIMBA cruise (crosses) as compared to the historical trip of the belgian BELGICA Expedition (squares). Framed is the region of the BELGICA wintering. The blue square marks the position of the launching of the Belgian metocean buoy (map: M. Vancopenolle).

were those have never been achieved.
There was also a specific politico-historical dimension for us to contribute to the cruise, since it took place in the same exact area where the Belgica expedition was forced to wintering, as it was trapped within the sea ice cover at the turn of our century (Figure 1). It is also for this very reason that our Chief Scientist has kindly suggested that the Station be called “Station Belgica” and that the names of the two major process stations be those of the home town of two of our Universities, Brussels and Liège. The cruise was also a unique opportunity for 6 of us, young scientists, to make their first encounter with the polar environment and support their ongoing thesis work with material they have collected themselves. In this regard too (as there are many other reasons), is the SIMBA project a true IPY endeavour.
As will be demonstrated below, the cruise has been a fantastic success, given its considerably shortened duration. We managed to drive our initial “core” project to more than 80% of success, with exciting results that already indicate a very good choice for the sampling sites. We were also very lucky that the chosen floe did not disintegrate during the whole experiment, allowing us to revisit each of our two process stations at 5 regularly spaced intervals, in the course of nearly four weeks.
Table 1 here below gives an idea of the amount of work achieved during our stay at Station Belgica:

Samples	**Number of samples collected**
Ice cores	162
Sackholes	136
Temperature	353
Salinity	707
$\delta^{18}O$	485
Structure	22
DMSx	800
Water Filtration for Iron	436 l.
Bell CO_2 fluxes	84
particulate and dissolved organic matter (POC and DOC)	240
particulate and dissolved saccharides	240
particulate and dissolved uronic acids	128
transparent exopolymeric particles (TEP)	240
dissolved free amino acids (DFAA	240
Chla (melted as is)	249
Chla (in Filtered sea water) – 2 fractions 0.8 and 10 μm	316
Preserved samples for organisms determination	145
Microscopic slides with glutaraldehyde	145
Bacteria: microscopic slides made from samples preserved with formaldehyde and stained with DAPI ; estimation of cell viability with sytox green dye	200
Nutrients	341
TD-Fe samples, DFe samples, PFe filters	183

Table 1: number of samples processed during the SIMBA cruise (Belgian team)

Apart from the “ core “ process ice stations we have run a series of side projects:

- Underway CO_2, in collaboration with S. Jacobs and co-workers
- CTD casts (including anthropogenic CO2 assessment)
- Trace Metal casts
- Way-In ice stations (short duration)
- New ice formation site, with active production of frost flowers

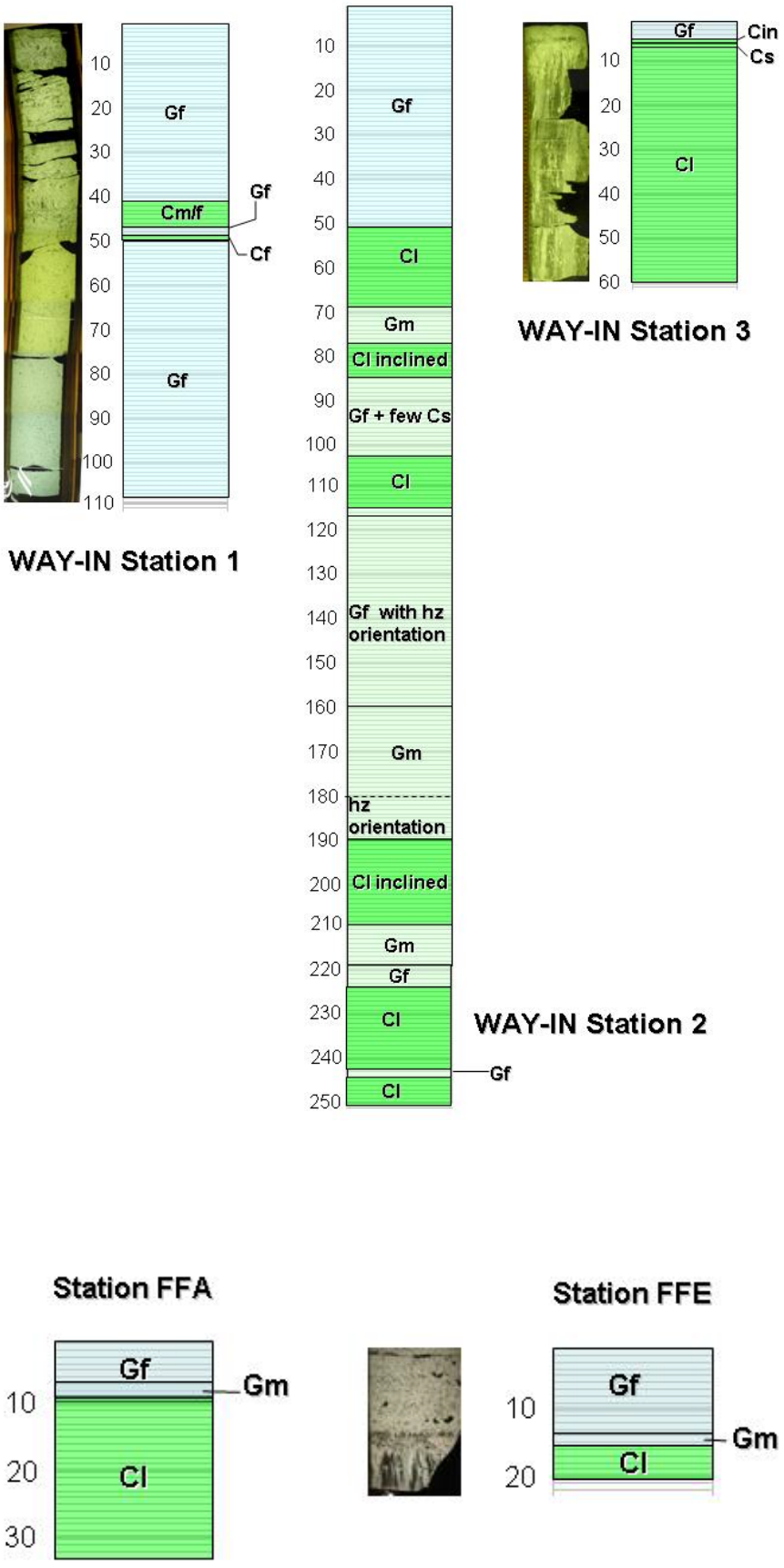

Figure 2: Summary of the textural properties of the ice cores at the WAY-IN (top) and Frost Flowers (FF, bottom) stations. For each: left = 2 mm thick section in transmitted light and/or under crossed polarizers, right = texture drawing. Key: G=Granular ice, C= Columnar ice, P= “Platy” crystals, vf= very fine, f= fine, m= medium, c= coarse or l= large, fs= frozen snow

The WAY-IN Stations

The initial project had foreseen regular sampling of daily ice stations, both on the Way-in and on the Way-out. For logistical constrains and considerable delay due to the fire declared on board early during the trip, we had to refocus our goals, and limit our “transect” studies to three stations on the way in, with limited sampling time (3 hours). These were also typically an excellent training for the longer term work to come at the process stations.
Figure 2 (top) gives an overview of the textural properties of the ice from the three Way-In Stations. Figure 3 shows the temperature and salinity profiles for those stations.

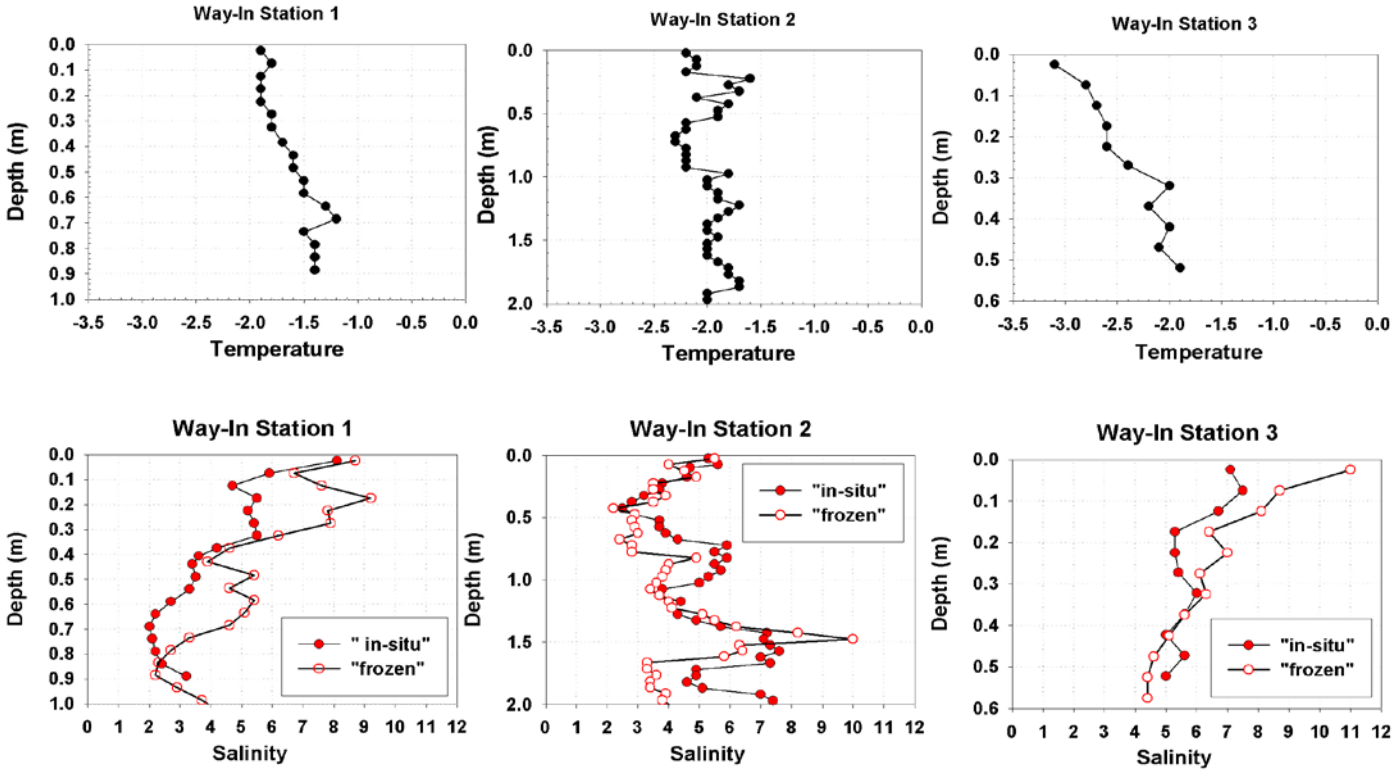

Figure 3 : Temperature and salinity profile at the 3 WAY-IN Stations

The three way-in stations show very contrasted structures. Stations 1 and 2 are typically granular, reflecting the dynamic environment of the marginal ice zone. Station 2 shows clear signs of rafting (inclined layers, oblique columnar inclusions, aligned layers of frazil…) that are confirmed by the fluctuations of the salinity and temperature records of figure 2 and 3 (low temperature-high salinity vs. high temperature-low salinity). The fact that these fluctuations are still detectable in the salinity and temperature profiles indicates that the rafting process is probably fairly recent. Station 3 is more typical of first year sea ice growing in calm conditions, with a dominance of columnar ice. The ice is always very warm, with slightly higher gradients in the southerly Station 3.
The salinity profiles are also very interesting, in that they show how profiles can differ under the combined effect of spatial variability and sampling procedure. The full circle curves correspond to samples cut and melted from one core “in-situ” and the open circle curves to samples from another core nearby (20 cm distance), immediately cooled down on retrieval (in a box with cooling bags at -25°C) and brought back frozen to the ship to be cut with a band saw and melted on board. There is no clear trend of desalination processes linked with the “delayed” salinity measurements. On the contrary, “delayed” salinities are generally higher where the largest discrepancies exist. Some limited contamination could have occurred from sea water refrozen in the storage bags, as attested by the single point peak

salinities at natural break (at 0.1 and 0.65 m in the Liège 1 core, for example). We have attempted to decontaminate the outer skin of another core to see if that would reconcile the observed discrepencies. To our surprise, it gave bulk salinities overall 1 to 2 mil lower than both other cores!...This suggests that both the “in situ” core and the “frozen” core retain brine in their outer skirt, which we get rid of when we decontaminate the outer few mm. In order to remain coherent with previous studies, we have decided to keep the two initial types of measurements we started with.
Cores from the three stations have been partly processed and partly stored for further measurements in the “home laboratories”. The approach will be similar to the one described in full in the following section. It is interesting to note that the rafted ice cover of Station 2 showed a few layers extremely rich in ice algae, generally corresponding to the frazil layers at the limit of individual rafts. On sampling and treatment, those layers were degassing strong emanation of what smelled like H_2S, not DMS.

The PROCESS Stations

Stations Set-up and suite of measurements

The Stations

Figure 4 gives a general overview of the two sites chosen for the process stations. These have been chosen during a first exploratory day trip on arrival on the Ice Station Belgica location. They were selected considering the following criteria:

- Homogeneity of surface properties (level ice, uniform snow thickness) to maximize our chances to address “simple case processes”
- Contrast in mean snow thickness, ice thickness, ice type (columnar vs. frazil), ice conditions (positive freeboard vs. flooding)
- Minimum extension area of 100m by 100m to ensure repeated visits (ideally 5) to each sites, in the allotted time on Station Belgica.

We will see below that these criteria were actually fully met.
We have set up a regular sampling schedule at each Process Station, so that we could also ensure proper treatment of the samples on-board. The cycles proceeded as follows:

- Day 1:visit Brussels
- Day 2: start processing Brussels
- Day 3:visit Liège
- Day 4 and 5: Processing Brussels and Liège
- Day 6: cycle restarts

On each site a “clean area” has been delineated with flags to prevent from accidental contamination (the main concern being our trace metals measurements), on an area of about 100m by 60m (Figure 4). At each Process Station, sub-areas of about 10x10 meters were delineated for each of the 5 visits. These were kept fairly close to each others, to limit the impact of spatial variability. Within those clean areas access was only permitted to people wearing tyvex clean suits and plastic bags around the shoes. However, the sites have been chosen so that a suite of other activities (geophysics, biology, meteorology, radiation balance…) could be run nearby on the same homogeneous piece of ice. Power supply was also located at least 100 meters away from the clean sampling area (a special power cord with a dedicated distribution box had been made for that purpose) to avoid CO_2 contamination of the samples and flux measurements from running the generator. For the same reason, the base camp and cargo download areas associated to each area were

settled at a similar distance. On a larger scale, the location of the process stations have been chosen as far as reasonably possible from the ship, that is between 1 and 2 km away from it.

Sampling strategy at the field stations

We have established a common sampling protocole for each of the Process Stations, as illustrated at the center-bottom of Figure 4. As an initial step, the pristine surface was sampled for snow by a single operator, at the center of the dedicated area. Then a first hole would be drilled through he sea ice cover. The resulting core (core TS) was dedicated to in-situ temperature and salinity measurements. As quickly as possible following the extraction, the ice core was placed on a working table and point temperature measurements were operated at a 5 cm resolution, drilling a small hole of the exact diameter of the digital probe meter perpendicular to the sides of the core. A fast adjusting thermometer was chosen for that purpose, and the measurements regularly cross-calibrated with another digital thermometer. Then the TS core was sliced into 5 cm salinity slices that were stored in ad-hoc sample containers and left to melt. The hole resulting from the TS core drilling was immediately used for sea water sampling at three reference depths: ice-water interface, 1 meter water depth and 30 meter water depth. The water were collected using a peristaltic pump, specially equipped to work in cold conditions, and a Gardena tubing device that was tested to be non-contaminant for trace metals. On these waters, we perform the same suite of measurements as those made on the sea ice and brine samples (see below).
Then a series of ice cores was retrieved, regularly spaced at 20 cm intervals, dedicated to the multi-parametric measurements listed in Table 2 here below:

Measurements	Core codes
Temperature, Salinity “in situ”	TS
Total gas content, O_2, N_2, CH_4, Argon	G1
CO_2	G2
DMS, DMSP, DMSO, thin sections	DS
First half: 5-cm resolution for Chla (melted “as is”), Salinity “frozen”, $\delta^{18}O$, Nutrients*; Second half*: 10-cm resolution for Chla (melted in Filtered Sea water), organisms determination)	SBio
Calcium carbonate extraction and characterization (concentration, type), Carbonate chemistry (Alcalinity, pH, DIC) on centrifuged ice samples	Ca
Organic Matter (6*10cm levels)	Bio3
Bacteria counts, viability	Bio4
Integrated Top/Bottom for all variables (mean values)	TB
Carbonate chemistry (Alcalinity, pH, DIC) on melted ice samples	KJ
Iron concentrations (Total, Dissolved, Dissolvable, Particulate) 6*10 cm	I1
Iron isotopes	I2
Iron incubation material	I3

Table 2: Assignment of Process Station cores to specific measurements

While ice cores were retrieved, Bell CO_2 flux measurements were performed randomly, both at the snow surface and at the ice surface. The accumulation chamber (West system®) is a metal cylinder closed at the top (internal diameter 20 cm; internal height 9.7 cm) . A rubber seal surrounded by a serrated-edge iron ring ensured an air-tight connection between the base of the chamber and the ice. For measurement over snow, an iron tube was mounted at the base of the chamber to enclose snow down to the ice and prevent lateral advection of air through the snow. The chamber was connected in a closed loop between the air pump (3 L min^{-1}) and the IRGA of the SIES. The measurement of pCO_2 in the chamber was recorded every 30 sec for at least 10 min. The flux was computed from the slope of the linear regression of pCO_2 against time ($r^2 \geq 0.99$) according to Frankignoulle (1988).

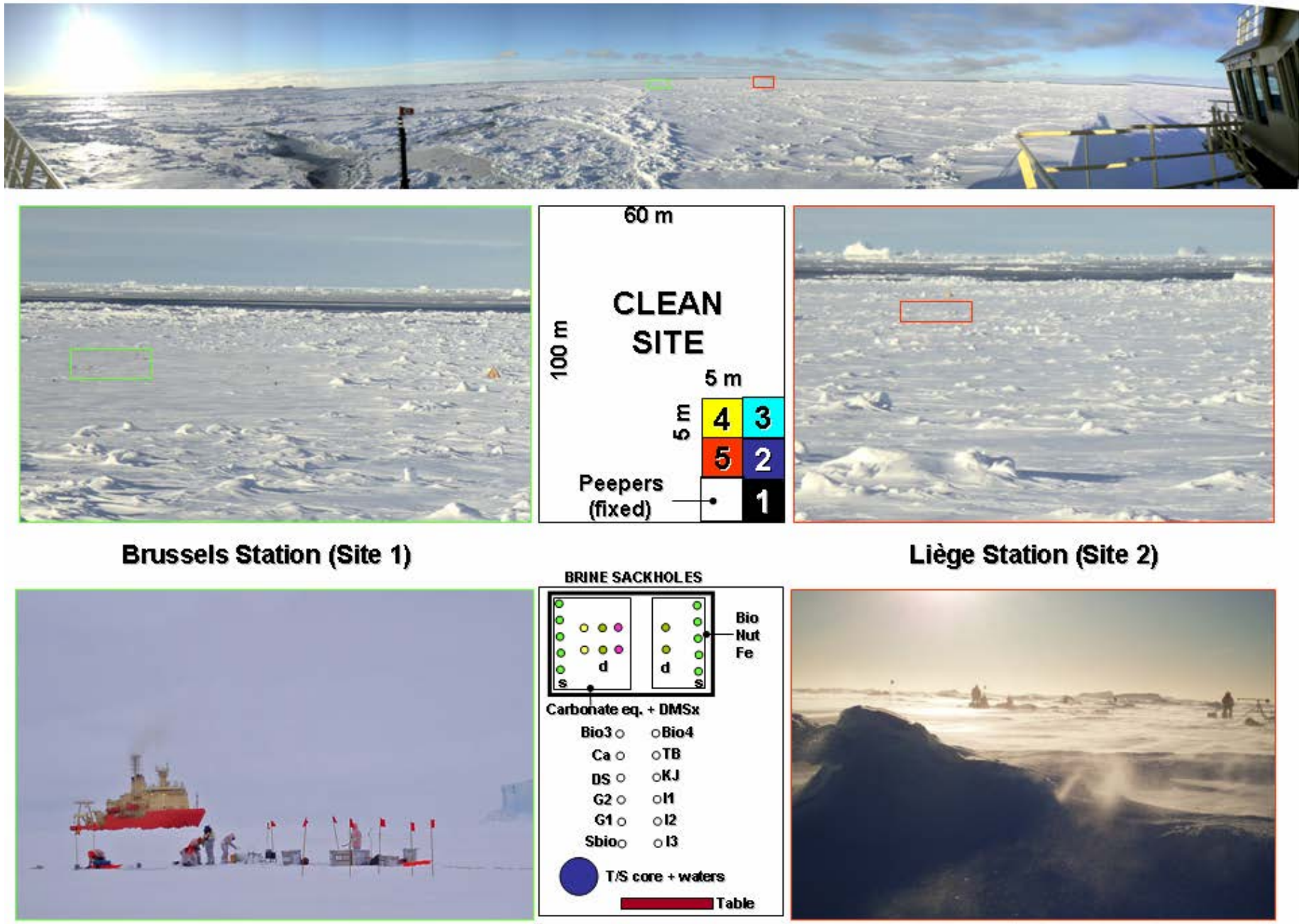

Figure 4 : General overview of the two sites chosen for the process stations : site 1 (Brussels) and site 2 (Liège). Top: panoramic view of the Northern section of the floe from the bridge, Middle: enlargement of the Brussels (left) and Liège (right) sampling sites, Bottom: general view of the working areas at Brussels (left) and Liège (right). The centre-top sketch illustrates the location of the areas chosen for the five successive sampling cycles at each process station. The centre-bottom sketch shows the (idealized) organisation of a given sampling site.

The uncertainty of the flux computation due to the standard error on the regression slope is on average ±3%. CO_2 fluxes values correspond to the average of three measurements.
Brines collection followed the ice core sampling. To collect the brines, sackholes (uncompleted coring) were drilled down to various depths into the sea ice cover, allowing gravity drainage of internal brines. Traditionally we choose those depths on the basis of the temperature profile: one above the -5°C (a rough approximation of the 5% brine volume permeability limit) and the other below it.
In this case, since nearly all ice temperatures were above -5°C, the levels were arbitrarily chosen at -15 cm (shallow brines) and -40 cm at the Brussels site (mean thickness 55 cm) and -15cm and -60 cm at the Liège site (mean thickness 100 cm). Those levels were sampled in detail for all the parameters, including those related to the study of the carbonate system, as described in further detailed here below:

pH of brines (sackholes) and water column

pH was measured on board using commercial combination electrodes (Ross type, Orion®) calibrated on the total hydrogen ion scale using TRIS (2-amino-2-hydroxymethyl-1,3-propanediol) and AMP (2-aminopyridine) buffers prepared at salinities of 35 and 60 according to the formulations proposed by the DOE (1994). pH measurements were carried out as soon as possible after sampling to the laboratory (typically less than 3 h after sampling on the ice station, within 30 minutes after sample collection from the rosette), and samples were maintained at low yet non freezing temperature (typically between 2°C and 7°C) until measurement. The pH electrode was calibrated at temperatures ranging from 2°C to 7°C, at salinities of 35 and 60. The accuracy of pH measurements was ±0.01 pH units.

Total alkalinity (TA) of brines and water column

Sample for TA measurements were filtered on GF/F glass filters within 3 hours after sampling. TA was measured on board at the laboratory temperature within one day after sampling using the classical Gran electrotitration. The reproducibility of measurements was ±4 µmol kg^{-1}. Measurements of TA in Certified Reference Materials, distributed by A. G. Dickson of Scripps Institute of Oceanography, were conducted and appropriate corrections were made to the data.

Dissolved inorganic carbon (DIC) of brines and water column
Values of DIC reported in this report were calculated from pH and TA measurements with the CO_2 acidity constants of Mehrbach et al. (1973) refitted by Dickson and Millero (1987) and other constants advocated by the DOE (1994). However, samples for DIC measurements were collected at each "Bruxelles" and "Liège" ice stations and several rosette casts (see table below). These measurements will be carried out in our laboratory using a new system "AIR-DIC" developed by Marianda® that allows measurement on low volumes (less than 20 ml). This feature can allow DIC measurement from brines extracted from ice cores extracted by centrifugation.

Oxygen
Dissolved oxygen were also measured at each "Bruxelles" and "Liège" ice stations within brines and underlying water, and from samples collected on several rosette casts (see table below) using the classical Winkler method. In addition, oxygen was also measured at several "Bruxelles" and "Liège" ice stations using an Aanderaa® 3835 oxygen optode.

A major concern throughout the whole sampling procedure has been to prevent contamination in trace metals, especially iron. Nitrile gloves were used for handling the iron dedicated samples, and items used for sample collection and storage were acid-cleaned and

sealed in plastic bags. The snow was collected with a polyethylene ice shovel into a 10L polyethylene container. The 14 cm diameter electropolished stainless steel core barrel (Lichtert Industries, Brussels, Belgium) has been specially designed and tested to be non-contaminant for iron. Seawater was pumped up with a portable peristaltic pump (Cole-Parmer, Masterflex E/P) and trace-metal clean tubing and collected in 2L polyethylene bottles. For interface and 1 m waters Masterflex silicone pump tubing was used, and transparent braided PVC tubing for 30 m. Finally, the sea ice cores dedicated to iron determination were immediately packed in acid cleaned plastic bags and stored at minus 25 degrees Celsius.
Close to the area dedicated to the first cycle on each site, a battery of 10 peepers (devices to measure "in situ" pCO_2 in the ice) was inserted initially into the sea ice cover at various depths. Details on these measurements will be found in the specific section by K. Johnson.
Also multi-point line and point radiation balance measurements were performed by M. Vancopenolle. These are reported elsewhere in a dedicated section of this document.
As a whole, a full station would take approximately 12 hours of continuous activity on site, for 5 to 7 people.

On-board measurements

Once collected, the ice cores and water/brine samples were brought back to the ship in the course of the day, depending on skidoo shuttles available. There, pre-treatment or further direct measurements took place, as summarized here below:

- Ice cores textures cutting: 2mm thick sections to visualize ice crystals and inclusions
- Ice cores samples cutting for: salinity "frozen", Chla, nutrients, organic matter, bacterial counts, algae and bacterial viability, DMSx, Calcium carbonate filtering…
- Salinity measurements (conductimeter)
- $\delta^{18}O$ sampling
- Filtration for Chla and Nutrients analyses
- Nutrient analysis
- Ice cores sub-sampling for iron over six depth intervals of 10 cm, chosen in function of ice texture and Chl *a* distribution, using a carbon-steel ice saw and a titanium decontamination chisel to remove the possibly contaminated outer few mm of the ice core section
- Snow and water samples processing for iron concentration measurements in a class 100 clean van: Snow was melted at room temperature. Snow melt water, brine and seawater samples were filtered across 0.2 μm pore size 47mm diameter polycarbonate membrane filters in a polycarbonate filtration apparatus (Sartorius) with Teflex O-rings (Eriks, Alkmaar, Netherlands) under gentle vacuum (<0.5 bar). Filters were collected in polycarbonate Petri dishes and stored at minus 20 degrees Celsius. Of each sample, 250 mL sub-samples for total dissolvable iron (TD-Fe, unfiltered) and dissolved iron (DFe, filtered) were collected, and acidified to pH = 1.9 (1mL acid per liter of sample) with subboiling distilled ultrapure 14M nitric acid (HNO_3)
- Snow and water processing for iron isotopes measurements in a class 100 clean van: Interface seawater sample was filtered on-board across a 0.2 μm pore size 142mm diameter polycarbonate membrane filter in a polycarbonate filtration apparatus (GeoTech) using the portable peristaltic pump. The filtrate was acidified to pH 1.9 and the filter stored at minus 25 degrees Celsius.
- Fixation of samples for organisms determination, bacterial counts and viability
- Alkalinity, pH, dissolved oxygen on the water and brines (see specific section)

On-board experiments

In addition to field sampling, several on-board experiments were performed with two main foci:

a) Lability of organic matter

These experiments were performed in 2 occasions: at Station Brussels 1 and Brussels 5. Three types of experiments were conducted, corresponding to three different media:

- organic matter and bacteria from seawater 0m
- organic matter from brines and bacteria from seawater 0m
- organic matter and bacteria from sea ice

Bioassays were incubated in the dark, at -1,1°C and followed up for a period of 10 days. Regular sampling has provides 140 samples for dissolved organic matter and dissolved saccharides and 70 samples for abundance and biomass of bacteria

b) Incubations for iron availability in the presence of organic ligands

Short incubations were performed 3 times at the Brussels Station (Bxl-3, Bxl-4 and Bxl-5) and *Long incubations* were performed twice at Brussels Station (Bxl-4 and Bxl-5).

Short incubations: Two types of media were considered for the short incubation experiments:

1. sea water collected at 0m depth
2. filtered sea water with addition of melted bottom sea ice

In each case, 6 different treatments were applied to the sea water:

1. Control (without addition of Fe and organic ligand)
2. addition of Fe (1nM)
3. addition of Desferrioxamine B (60nM) + Fe (1nM)
4. addition of Protoporphyrin IX (60nM) + Fe (1nM)
5. addition of Glucuronic acid (60nM) + Fe (1nM)
6. addition of Alginic acid (60nM) + Fe (1nM)

After addition of the different organic ligands, samples were incubated at -1.1 °C during 16 to 20 hours.

After incubation, 200 ml was filtered on filters with different cut-off sizes (10, 0.8 and 0.2 µm) in order to measure the total iron uptake.
We have also collected dissolved samples (<0.2 µm) to measure the remaining iron in the dissolved fraction. A part of these samples was ultrafiltered on Anotop filters of 0.02 µm cut-off size to measure the predominant size fraction of iron.
A solution of oxalate was added to the remaining 800 ml, and after 20 minutes, samples were filtered on filters with different cut-off sizes (10, 0.8 and 0.2 µm) for measuring the intra-cellular iron uptake.

Parallel incubations of 14C were performed on the control and the '+Fe' samples in order to estimate the primary productivity. After addition of 14C, samples were

incubated at -1.1°C during 16 to 20 hours, and then filtered on 10 and 0.8 µm filters.

Long incubations were also performed in order to estimate the long term effect of the addition of different organic ligands on the bioavailability of iron.
In this case, the different organic ligands were added to 4L of sea water, and the samples were incubated on the deck incubator during 3 days. After 3 days, a protocol similar to the one described above has been applied to the samples.

Preliminary results

Textural contrasts and visual ice properties

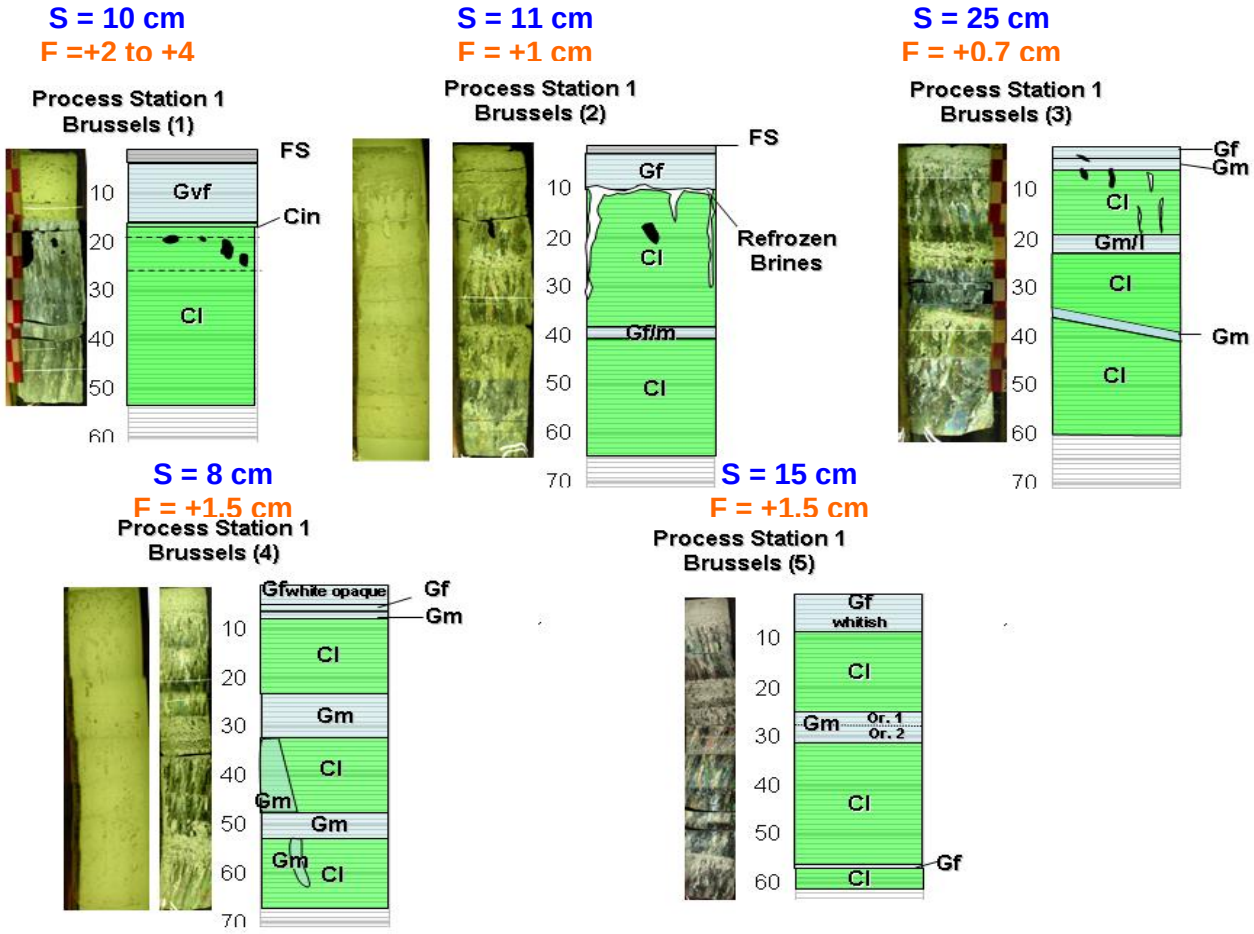

Figure 5 : Summary of the textural properties of the ice cores collected for the five sampling cycles (core Sbio) at the Brussels (site 1) process station. For each cycle: left = 2 mm thick section in transmitted light and/or under crossed polarizers, right = texture drawing. Key: G=Granular ice, C= Columnar ice, P= "Platy" crystals, vf= very fine, f= fine, m= medium, c= coarse or l= large, fs= frozen snow. Note the conspicuous brine tubes at Brussels (2), on the transmitted light section

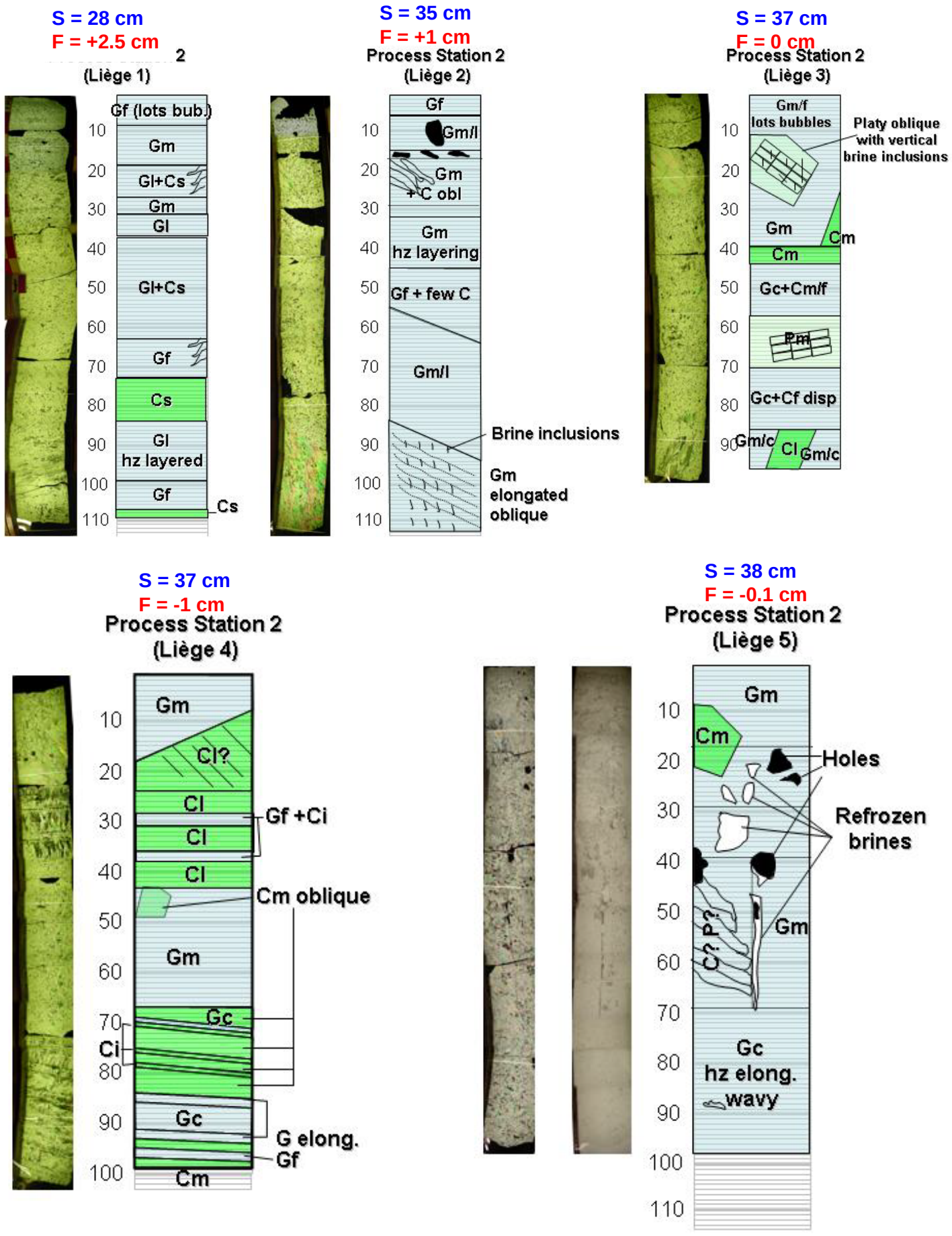

Figure 6: Summary of the textural properties of the ice cores collected for the five sampling cycles (core Sbio) at the Liège (site 2) process station. For each cycle: left = 2 mm thick section in transmitted light and/or under crossed polarizers, right = texture drawing. Key: G=Granular ice, C= Columnar ice, P= "Platy" crystals, vf= very fine, f= fine, m= medium, c= coarse or l= large, fs= frozen snow

Figures 5 and 6 summarize the textural characteristics of the ice cover respectively at the Brussels and the Liège location, for the duration of the experiment. Here, we confirm the strong contrast that exists between the two locations. The Brussels Station is 50- 70 cm thick, essentially made of columnar ice, with a variable number of thin granular inclusions and a 10-15 cm of granular fine ice at the top, a typical texture of first year ice grown in relatively calm conditions. The very fine grained whitish opaque top layer is probably mainly snow ice, but this will have to be confirmed by the $\delta^{18}O$ measurements. The sea ice cover is overlain by a moderately thin snow cover of 8 to 25 cm, and has shown a positive freeboard (0.7 to 4 cm) for the whole period. In the many thick sections and cuttings processed, no single brine channel structure was to be seen in the columnar ice. Instead, large tubes of refrozen brine inclusions were often seen to initiate at the top granular/columnar interface and to find their way to the bottom of the sea ice cores. This is clearly illustrated in the Brussels 2 transmitted light picture of figure 5, as well as on the half core cuttings and the 1 cm thick sections of Figures 7 and 8 respectively.

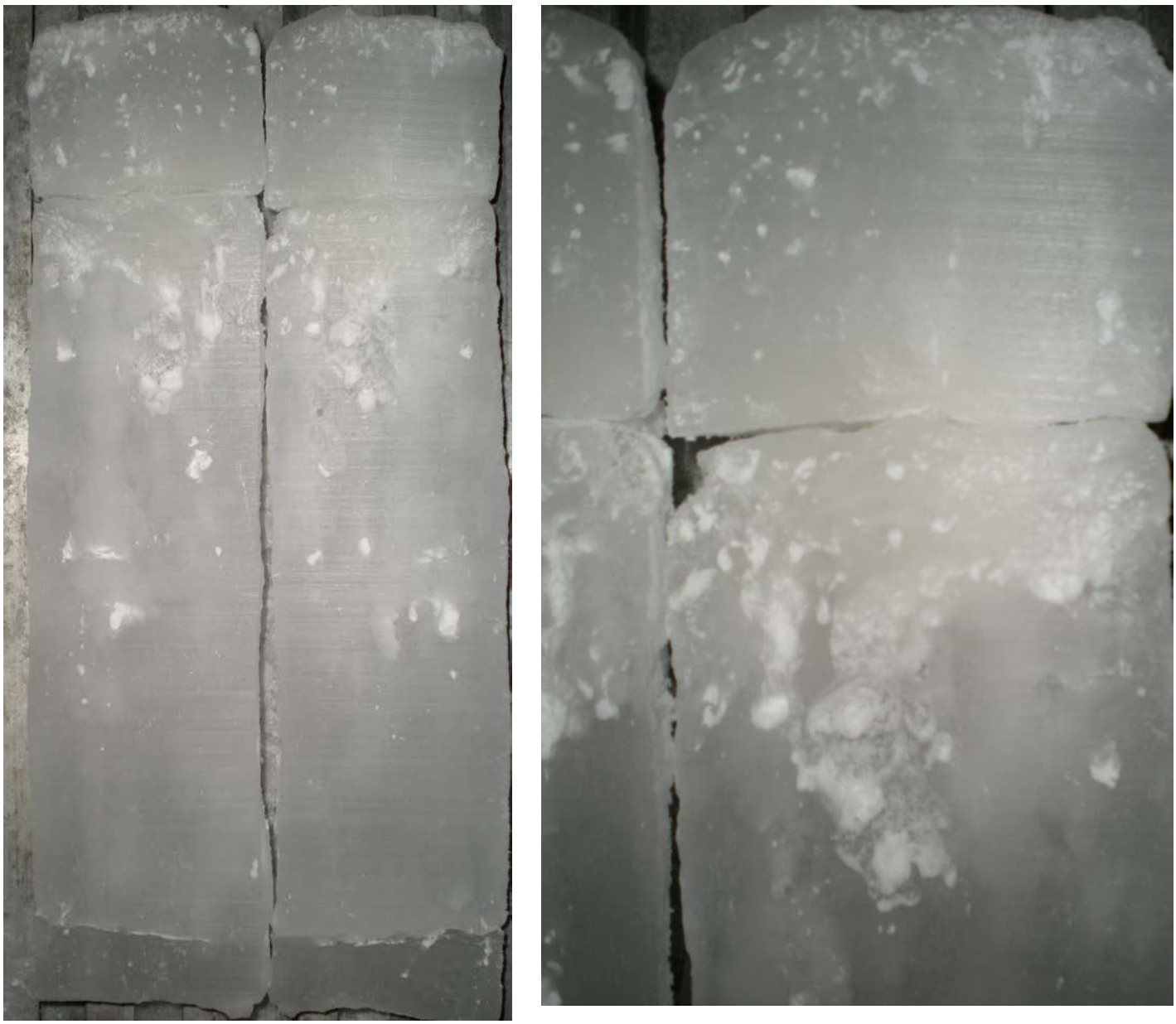

Figure 7 : Half core sections of the Brussels 3 Bio3 core. Note the white refrozen brine accumulated at the granular/columnar boundary and the long refrozen tube inclusions (seen whitish in transparency) that extend towards the bottom end of the core. Right: enlargement of the top part.

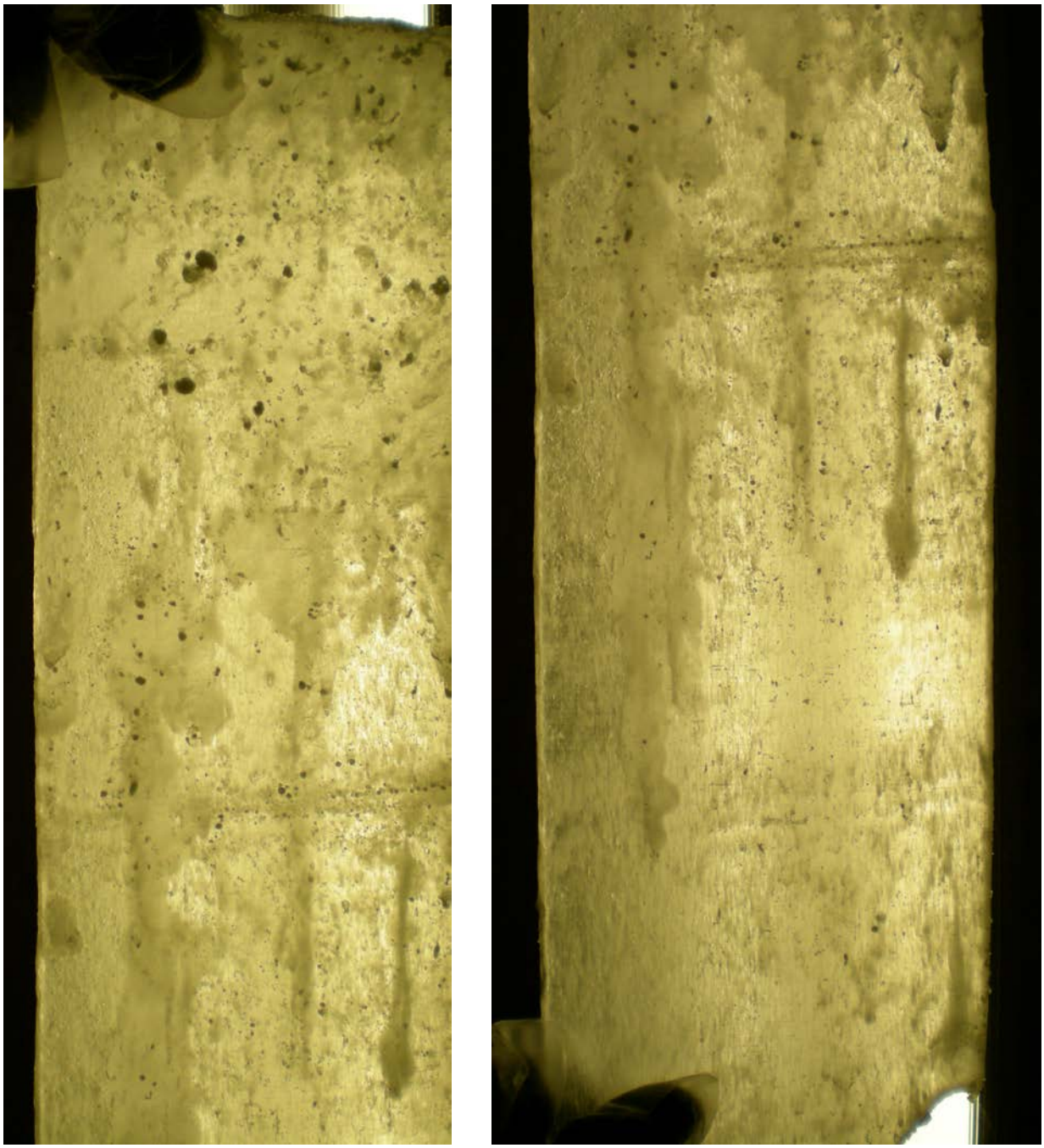

Figure 8 : 1 cm-thick section of the Brusels 4 core clearly showing the descending refrozen brine tubes. Fingers for scale.

The Liège Station shows a very different ice texture (Figure 6): the ice is there predominantly granular, with a large grain size variability and numerous facies disturbances suggesting essentially a dynamic origin with potential rafting events. The ice is also thicker (between 90 and 120 cm). Snow thickness is higher (28-38 cm) and the freeboard, initially positive, shows a clear trend towards flooding from cycle 3 onwards. Large brine inclusions are also frequent, but with a different geometry: large coalescent vacuoles rather than elongated tubes. One of them was present at the Liège 5 Station, but initiating somewhat at depth (about 40 cm down to 70 cm), apparently “exploiting” a strong textural boundary.
Generally, at both Stations, the ice appeared peculiarly “rotten” in its upper half, as illustrated by some examples in Figure 9. Note particularly the inverted funnel shaped cavity at the bottom of the core (lower right) that appears to connect to an internal channel.

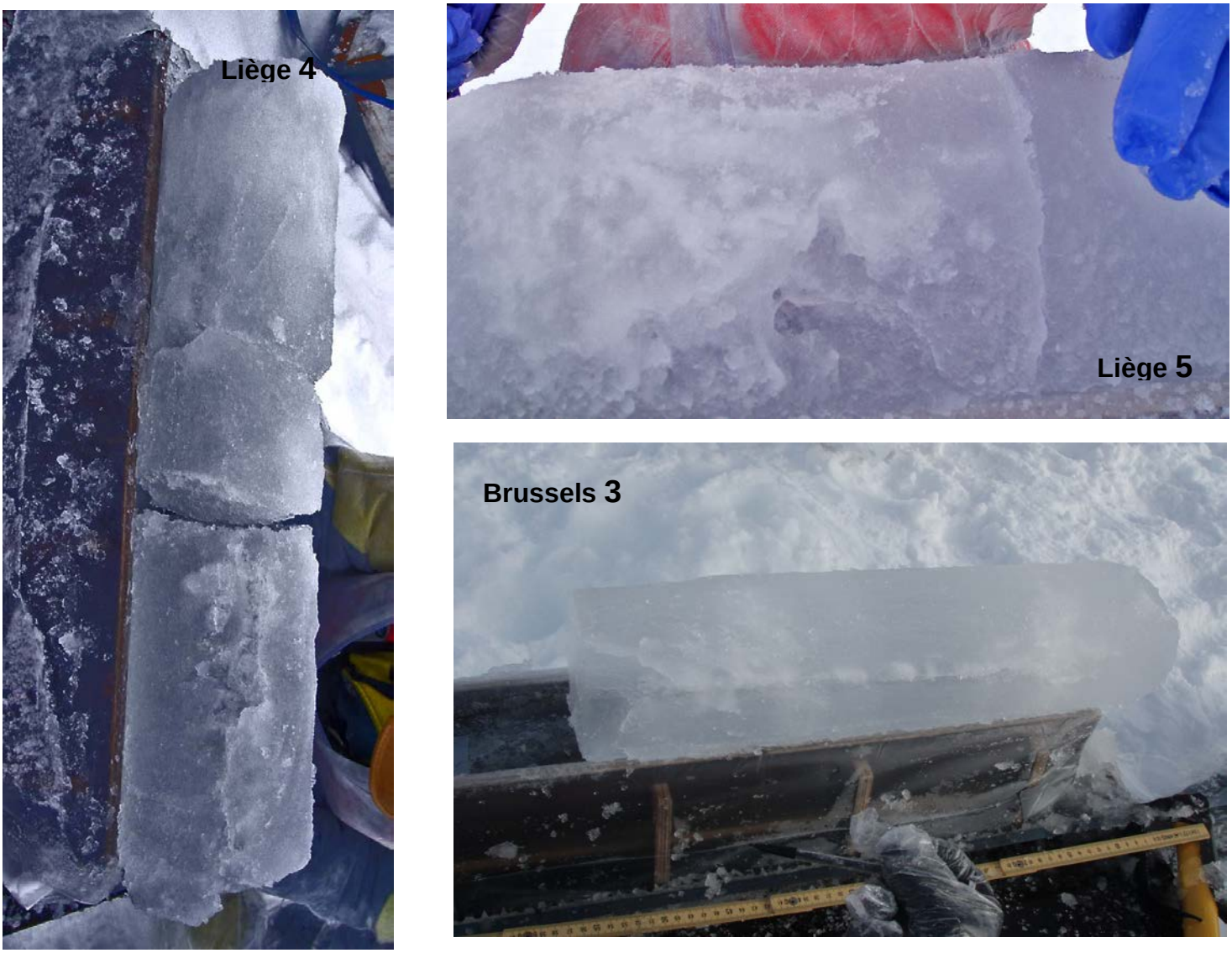

Figure 9 : Exemples from both Brussels and Liège stations of the state of degradation of the ice cores on extraction

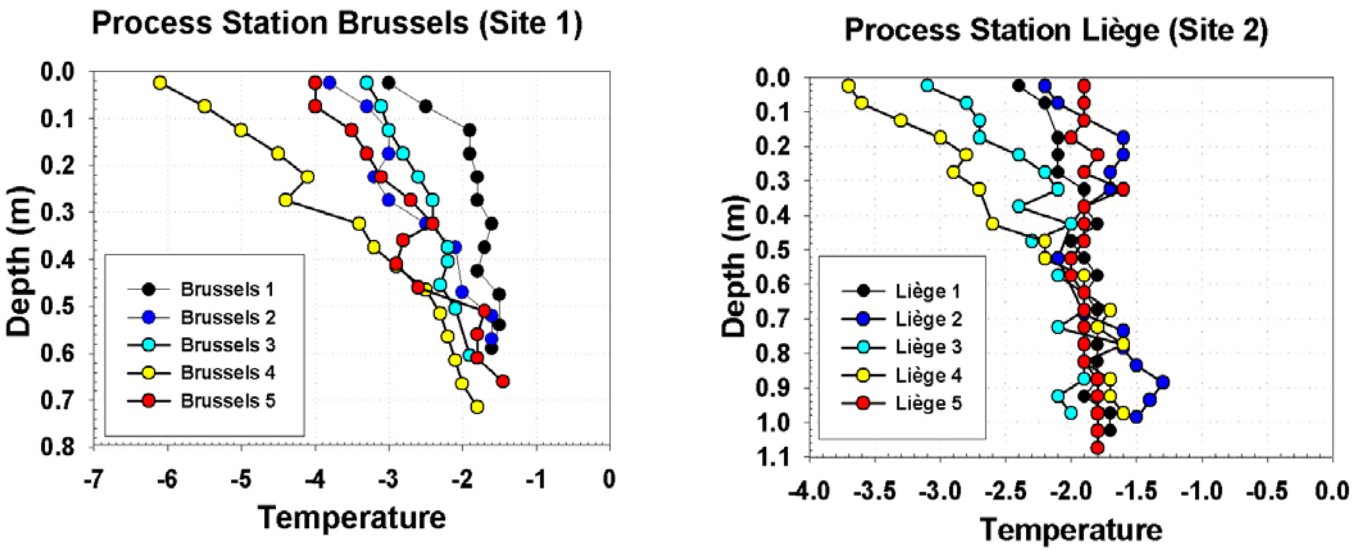

Figure 10 : Temperature profiles for the five sampling cycles at the two process stations

Temperature profiles

Figure 10 shows the evolution of the temperature profiles in the ice, at the two Process Stations. The trends are similar, although the range of the changes is somewhat dampened at the Liège station, because of the higher snow thickness. It somewhat reflects the synoptic evolution of air temperatures at “Station Belgica”, with an initially warm period, followed by a strong cooling (maximum at cycle 4) and a final warming (cycle 5). The ice is very warm initially in both cases, and close to isothermal, to the exception of the surface 15 cm, which probably started to record the cooling period. Note that, at the end of the observation period, Liège has recovered its initial temperature profile.

Salinity profiles

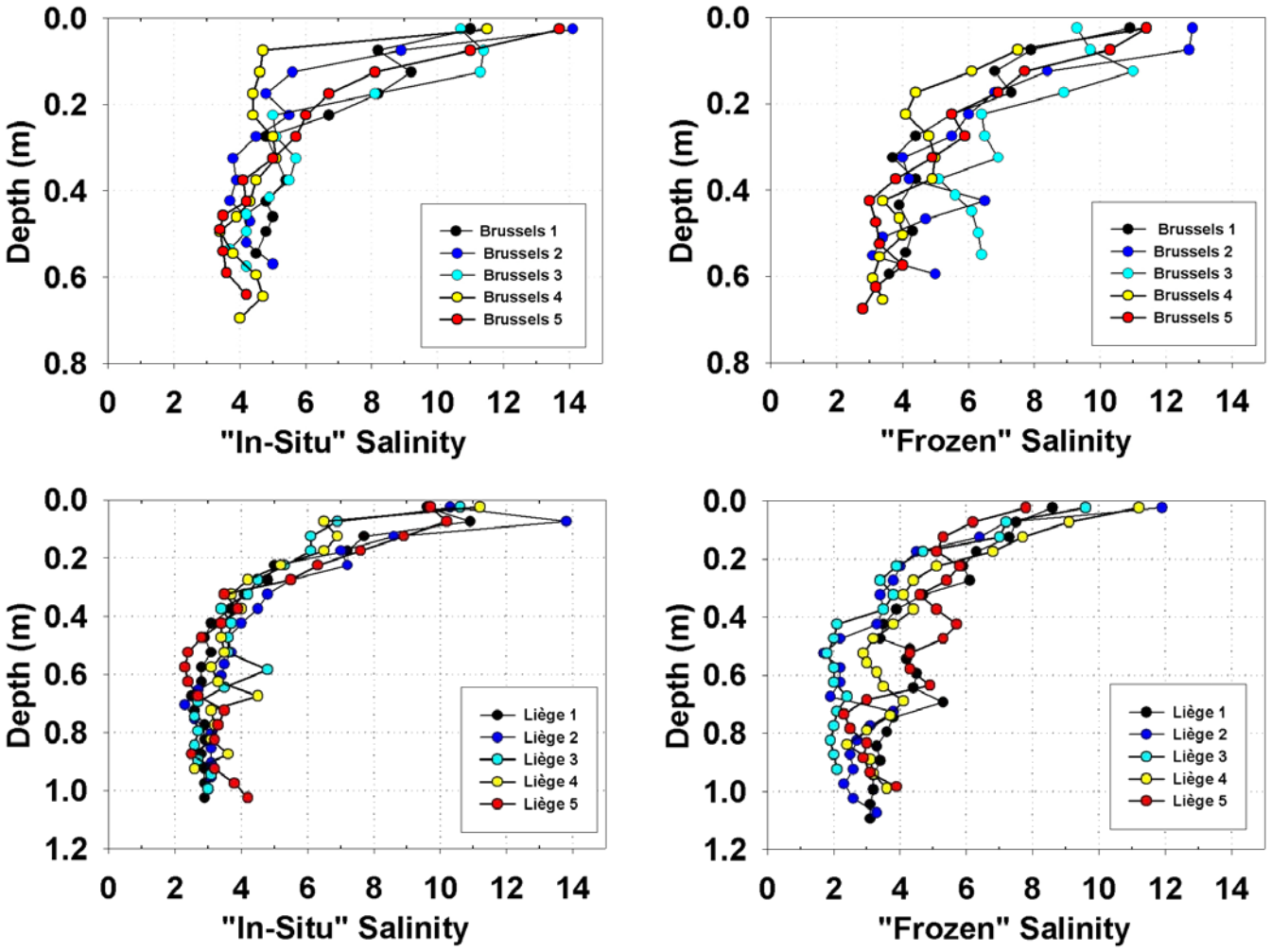

Figure 11 : « In situ » (cut on site) and « frozen » (cooled on site directly on extraction and cut in cold room on ship) salinity profiles for the five sampling cycles at the two process stations

As described in the “sampling strategy” section, we have measured bulk ice salinities in two ways: a) direct cutting in the field (“in situ”) and b) immediate cool storage in the field and band saw cutting in the freezer van on board the ship, for all sites. Figure 11 therefore plots bulk salinity profiles using both methods. Although trends and ranges are similar between the two techniques, it appears that the “in situ” curves are generally much smoother, show less extreme values and generally slightly lower values. This could be explained if one considers that internal brine pockets will probably be better preserved with the “cooling” technique,

rather than with the “in situ” technique, where the ice is cut open at warm temperatures. None of the profiles show the basal increase of salinity which is typical of a growing skeletal layer. This is not surprising, since all observations reported a smooth undulous interface, witnessing an overall basal melting process.
At Brussels Station, the trend is towards a salinity maximum migrating downwards during the three first cycles. Then cycle 4 shows minimal values in the upper layer. The last cycle brings the salinity curve back to its initial position at the beginning of the experiment.
The Liège situation is less clear. The two salinity records are here rather contradictory. If we consider the “frozen salinity” record, there seem to be a considerable desalinization process occurring between cycles 1 and 2-3 over the whole profile. The “in situ” salinity profile however does not show much happening. As flooding is observed at the surface (cycle 4), salinities are increasing over the whole profile (again only visible on the “frozen salinity” profile). Then there is a decrease of the salinity in the upper part and an increase in the lower part.

Calculated brine salinities and brine volumes

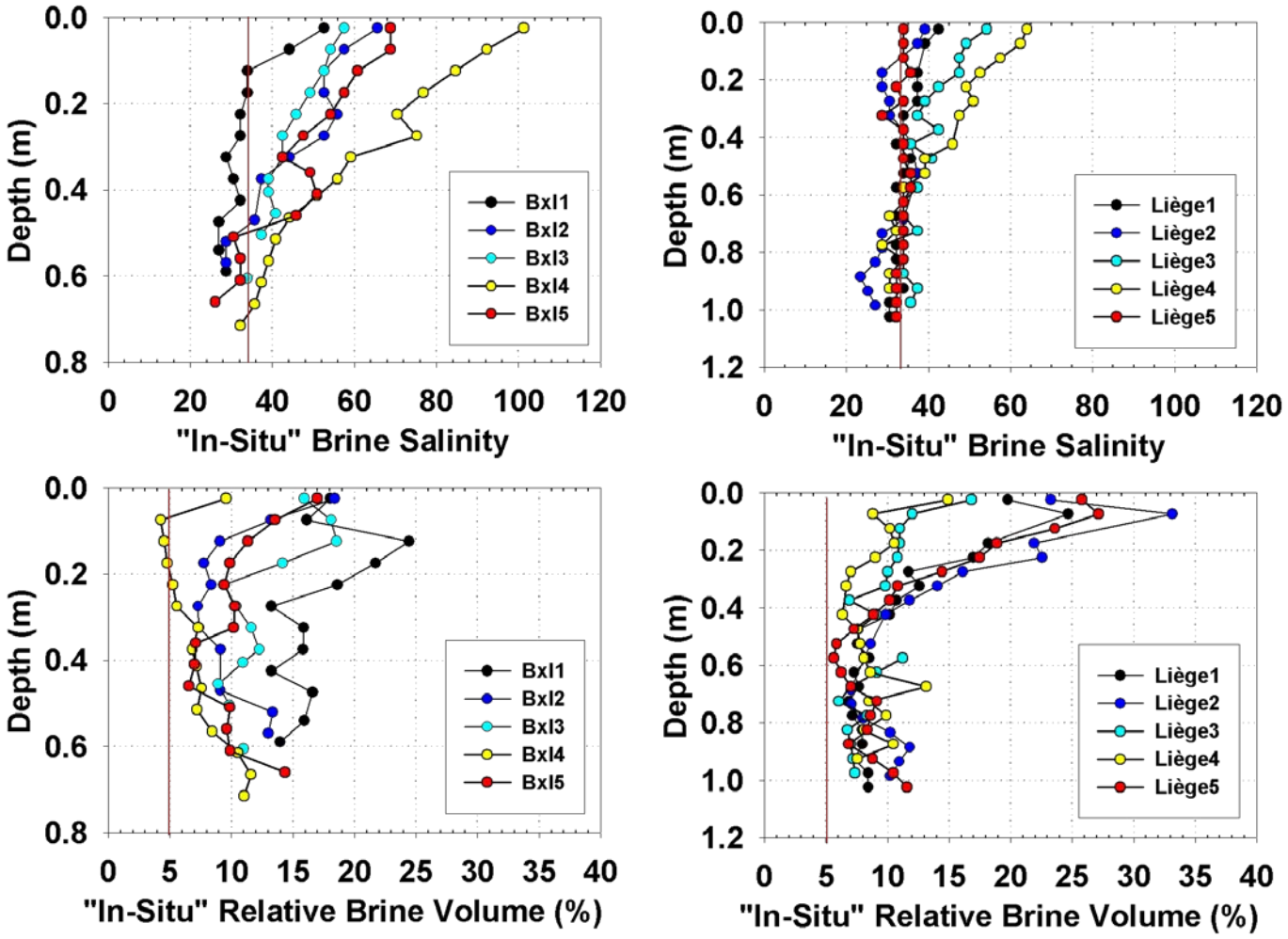

Figure 12 : Calculated brine salinities and brine volumes (using « in situ » bulk salinity values) profiles for the five sampling cycles at the two process stations

Calculated brine salinities strictly reflect temperature changes in the ice while calculated brine volume integrate both the temperature and bulk salinity effects. We have used here the

"in situ" bulk ice salinities for the calculations, since using the "frozen" bulk ice salinities would require a bit more work to insure depths compatibility between variables measured on two different cores. Table 3, here below lists the observed salinities in the shallow brine sackholes, together with the calculated value from the graphs of Figure 12.

Cycle	Brussels		Liège	
	Calculated Brine Salinity (17.5 cm)	**Observed Brine Salinity (15 cm)**	**Calculated Brine Salinity (17.5 cm)**	**Observed Brine Salinity (15 cm)**
1	33.9	36.7	37.4	38.2
2	52.5	65.7	37.4	46
3	49.2	64.1	47.52	45
4	76.8	86.4	57.48	65.4
5	57.5	66.1	33.9	40.7

Table 3: Comparison of calculated and observed brine salinities for the five cycles at the two process stations

The data agree fairly well, respecting the trends and relative levels and timings. Observed brine salinities are generally a bit higher, because they integrate the whole surface layer from 0 to 15 cm. Also, discrepancies are not surprising, given the fact that the brine holes were drilled a few meters from the TS core location. It was not rare to observe different behaviour (e.g. filling time) between brine holes on the same station. That variability is to be related to the microtopography of the snow-ice interface that typically consisted of bumps and troughs. The brine drainage into the sackholes as well as the potential flooding of the surface must have been partly controlled by these small scale effects.
Clearly, from these numbers and the top graphs of figure 12, it appears that the increase of brine salinities (starting from values close to sea water) in the surface layers proceeds with a different pace and to different maxima in Brussels (more dynamic) and Liège. This has to be linked with the relative importance of the snow cover thickness (and therefore heat fluxes to the atmosphere) at both sites.
Also, and for probably the same reason, the regular increase of brine salinity affects the whole of the sea ice cover at Brussels (60 cm) whilst only the upper 60 cm at Liège Station. Generally speaking, brine salinity profiles are initially at near equilibrium, then they get less and less stable during the first 4 cycles, with an enhanced gradient at Brussels. Cycle 5 brings the system back to equilibrium at Liège and lowers the gradient at Brussels.
Calculated brine volumes also behave very differently in terms of amplitude and timing between the two stations. Brussels is affected on its all depth whilst Liège only shows important contrasts in its upper half. At all times, but cycle 4 at Brussels, brine volumes are above the 5% permeability threshold of the "law of five" (Golden et al., 1998). The general pattern is to start with very high relative brine volumes (up to 25-30%), with a decrease with time from cycles 1 to 4. The latter is regular with time at Brussels and delayed until between cycles 2 and 3 at Liège. At both stations, brine volumes increase again for cycle 5. In the case of Liège, the profile returns to its initial values.

Preliminary interpretation of the evolution of the main physical parameters

It will certainly take much more thinking to understand the complexity and details of the observed sea ice system at the Station Belgica Process Stations, especially if one wants to dissociate small scale spatial variability (logistically constrained) from the temporal variability at a given location. However, some general pattern already emerges clearly. In terms of meteorological forcing, we were lucky to witness a full cycle of cooling and warming throughout the period, with large changes in the snow cover thickness, mainly driven by wind drift (although precipitations also contributed - see section on snow dynamics). This has resulted in major changes in brine salinities, drastically increasing the instability of the brine column in the initially very warm (isothermal) and porous sea ice, with initial brine salinities at

sea water value or slightly lower throughout. Incidently, this initial ice cover status is rather surprising so early in the season, although it had already been reported in earlier studies (e.g. Jeffries et al., 1995). Cooling of the surface layer has increased considerably the surface layer brine salinity. Since those brine are lying on top of very warm ice, thermodynamic equilibrium dictates that they will dissolve the underlying fresh water ice crystals to equilibrate at intermediate lower salinity and lower temperature. This will help transferring the "cold wave" downwards. Visual observation of descending brine tubes (not brine channels!) initiating at the granular/columnar interface in the cores, e.g. figures 6 to 8, obviously confirm this process. Bulk salinity profiles (especially the "frozen" salinity at Brussels) also illustrate temporal increases of salinity in the intermediate levels, followed by a general desalination at cycle 4. Finally, photographic documentation of localized brine "rain" at the underside of the ice cover show that brine actually exits the ice medium. Downwards transfer of brines in a porous sea ice cover should result in a counterbalancing upwards transfer of sea water, i.e. a convection process. We have direct and indirect indications that this process might occur, such as: a) funnel-like cavities connected to brine tubes at the bottom of cores (see figure lower right), b) excursions in the temperature profiles, c) microscale variability of temperature observed at a given level during the measurements and d) flooding at Station Liège, sustained by the snow loading. This then brings the whole system back to its original state, and potentially ready for a new event. The whole cycle has already been referred to in the literature as the "flood-freeze" cycle.

DMS/P profiles

We have collected about 800 DMS/P ice measurements during the cruise and these have shown a very dynamic system, in close connection with the physical evolution of the pack ice described above. Underlying surface waters and brines from sackholes were also sampled at both stations for all cycles. DMS/P was measured using the classical "purge and trap" technique on an AGILENT 6890 GC, equipped with a manual injection 6-way valve , a Restek packed Rt-xl-sulfur column and an FPD detector.

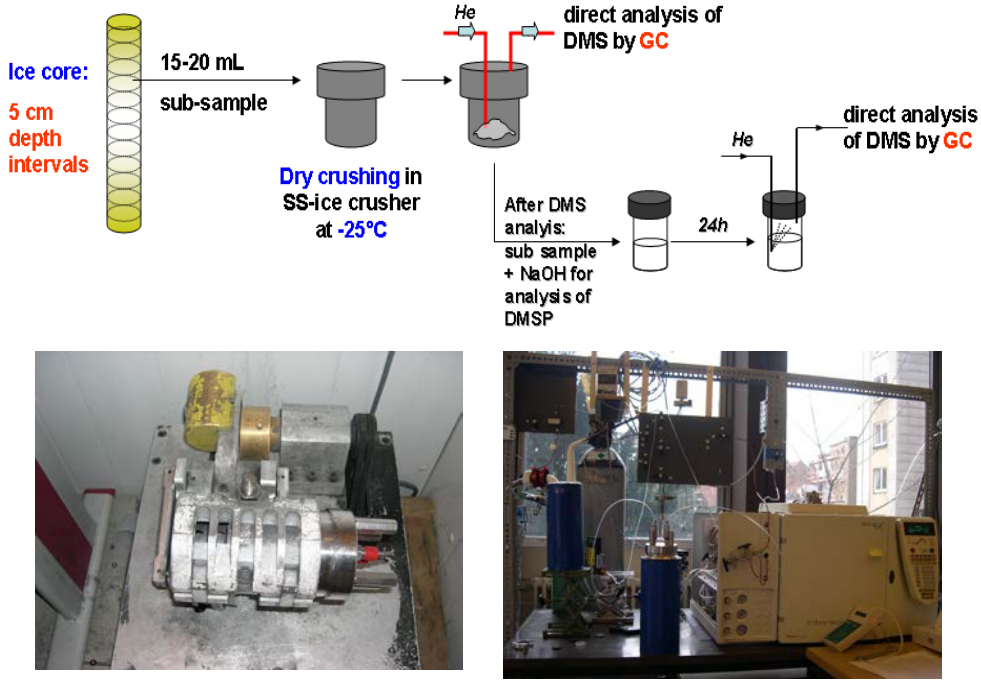

Figure 13 : The DMS/P analytical scheme applied for ice samples at the University of Brussels. A similar system has been used during SIMBA.

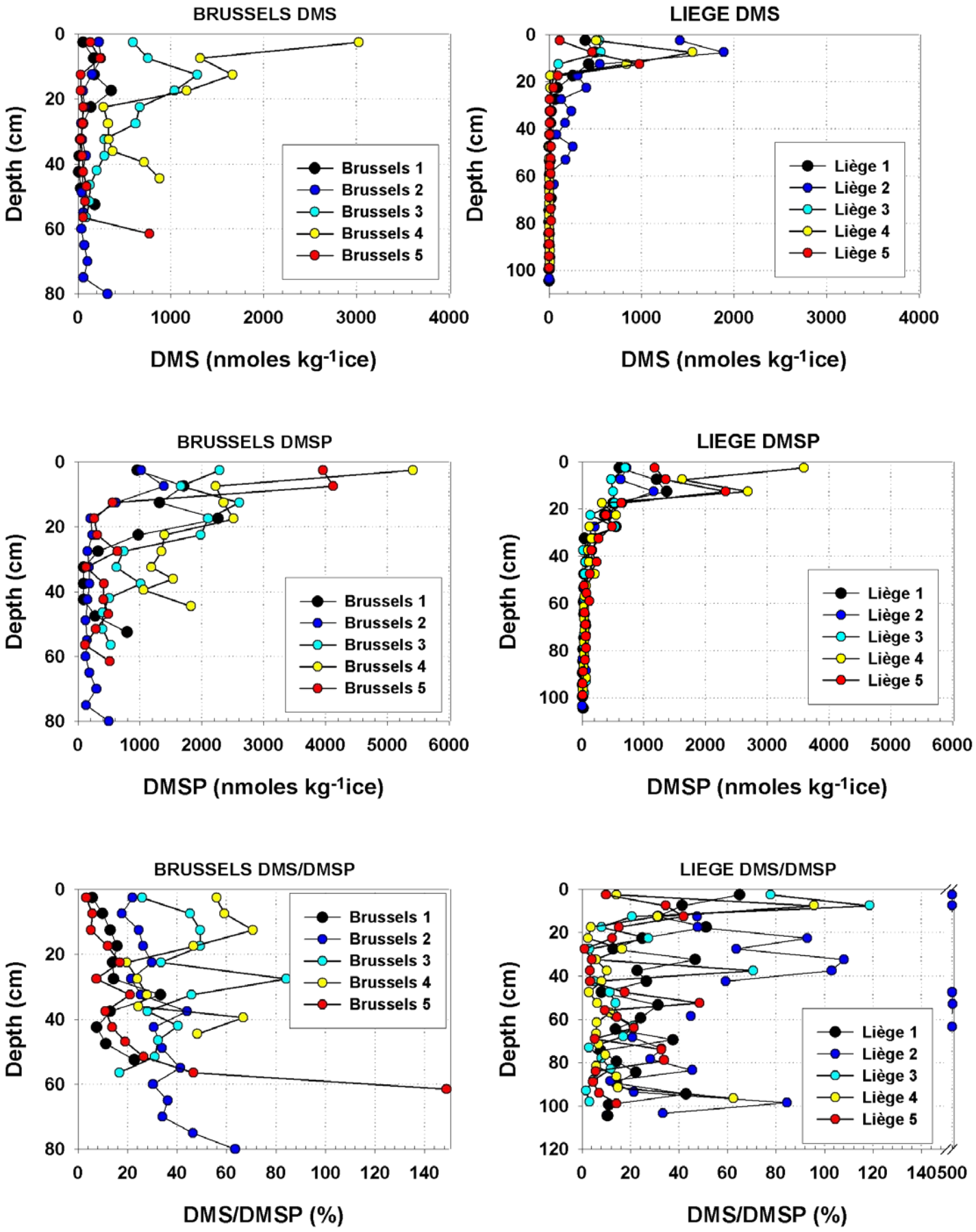

Figure 14 : DMS (top), DMSP (middle) and DMS/DMSP ratios in ice for the five sampling cycles at the two process stations

Ice samples were measured using a specific “dry extraction” technique (Figure 13), where the ice is crushed in a dedicated vessel into a fine powder, the headspace purged with Helium, trapped in liquid nitrogen, then released to the GC column. The powder is then collected and melted in the presence of excess NaOH, in order to convert the whole of the DMSP into DMS. The meltwater is then purged and trapped after 24 hours and sent to the GC column. This technique has been developed at the Université Libre de Bruxelles, in order to avoid potential bias on the DMS/DMSP ratios that was recently shown to happen when melting the samples in sea water.
Figure 14 summarizes the DMS/P and DMS/DMSP profiles results for the two process stations. The first striking feature is the general similarity of behaviour with the profiles for the physical parameters, with Brussels showing major changes in the whole ice column and Liège only showing major changes in its upper half. Another major finding is the highest recorded DMSP (5700 nM kg^{-1} ice) and DMS (3000 nM kg^{-1}) levels ever reported in ice (to our knowledge) so far, in the surface layer of Brussels Station on cycle 4. A third important preliminary finding, not shown on the graph, is that underlying sea water (1 to 30 meters) shows considerably high levels of DMS and DMSP (up to 30 nM), as compared to the usual sea water background of a fraction of nM in DMS. This corroborates the idea presented above of having active brine release to the underlying water column. A fourth highlight of these results is the clear trend for increasing DMSP and DMS levels in the surface layers from cycles 1 to 4, and a decrease back to initial levels for cycle 5. There is also a clear trend for invading lower layers in the course of time at Brussels Station. Finally, Brussels also shows slightly higher levels in the bottom layer. All these characteristics appear to be closely linked to the thermodynamical evolution of the sea ice cover and to the dynamics/speciation of the biological communities discussed in another section of this report. Of peculiar interest are the profiles of the DMS/DMSP ratios. Starting with relatively low values, apart from the bottom layer of Station Brussels, it considerably increases during the freezing event of cycles 3-4 and then returns to its initial values on cycle 5. This ratio, which is an indicator of the balance between DMSP production and lyasis will be discussed in full, to try separating algae metabolism and trophic relationships from purely physical convective or advective processes, once all the data are compiled.

pCO_2 profiles and CO_2 ice-air fluxes

We present hereafter only pCO_2 of sea ice brines (sackholes) and water column, and air-ice CO_2 fluxes.
Underlying water appeared to be supersaturated in CO_2 with respect to the atmosphere throughout the survey, with pCO_2 ranging from 404 up to 464 ppm. These values are consistent with underway measurements. In contrast, sea ice covers appeared to be under-saturated in CO_2 with respect to the atmosphere, ranging from 77 ppm at Liège site to 377 ppm at Bruxelles site. pCO_2 in brines "Liège" is always lower than at "Bruxelles" except at the end of the experiment. However, the overall temporal evolution is roughly similar at both station with an increase from the first measurement cycle (day 274- day 276) to the second (day 279- day 281), then a decrease between the second and third cycle (day 284 –day 286). An increase of pCO_2 lead to a maximum during the fourth cycle (day 289 –day 291) that is followed by a dramatic decrease leading to a minimum during fifth cycle (day 294-296). Several factors affect pCO_2 within sea ice, like temperature and salinity change, biological activity and precipitation/dissolution of calcium carbonate (Delille, 2006; Delille et al., 2007). Deciphering the influence of the different processes require further analysis using the data-set produced by the Belgian group. However we can note that the maximum of pCO_2 at "Bruxelles" site was observed on day 289, when convection brought sea water close to the surface with concommitent mixing of brines with high pCO_2 seawater. Such process has likely taken place at the Liège site, leading to a similar and simultaneous increase of pCO_2.

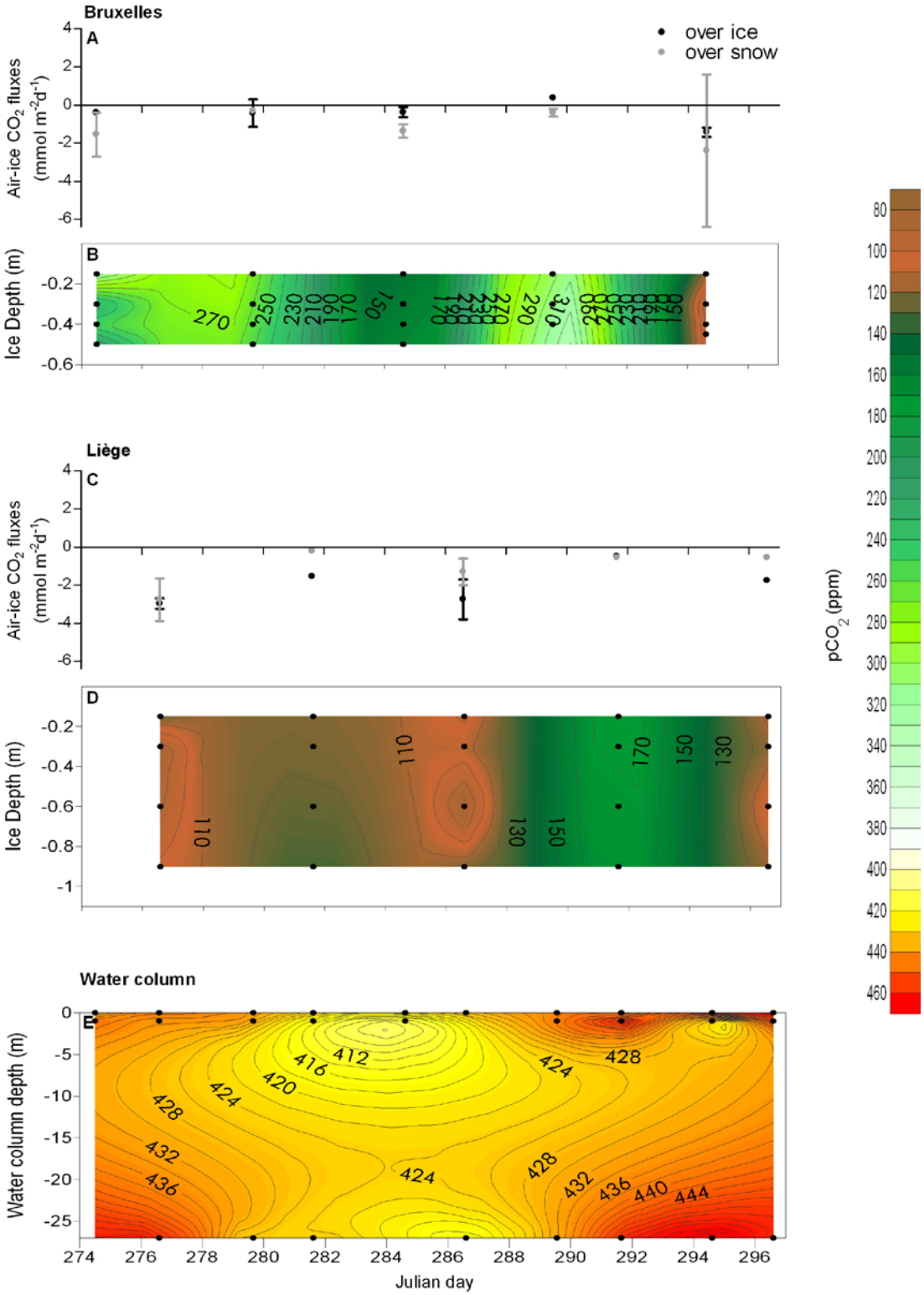

Figure 15: Temporal and vertical distribution of pCO_2 within brines at station Bruxelles (A), Liège (C) and within the underlying water (E) together with temporal evolution of air-ice CO_2 fluxes over ice (black dots) and snow (grey dot) at Bruxelles (B) and Liège (D). Bars represent the error derived from the difference of three replicate measurements.

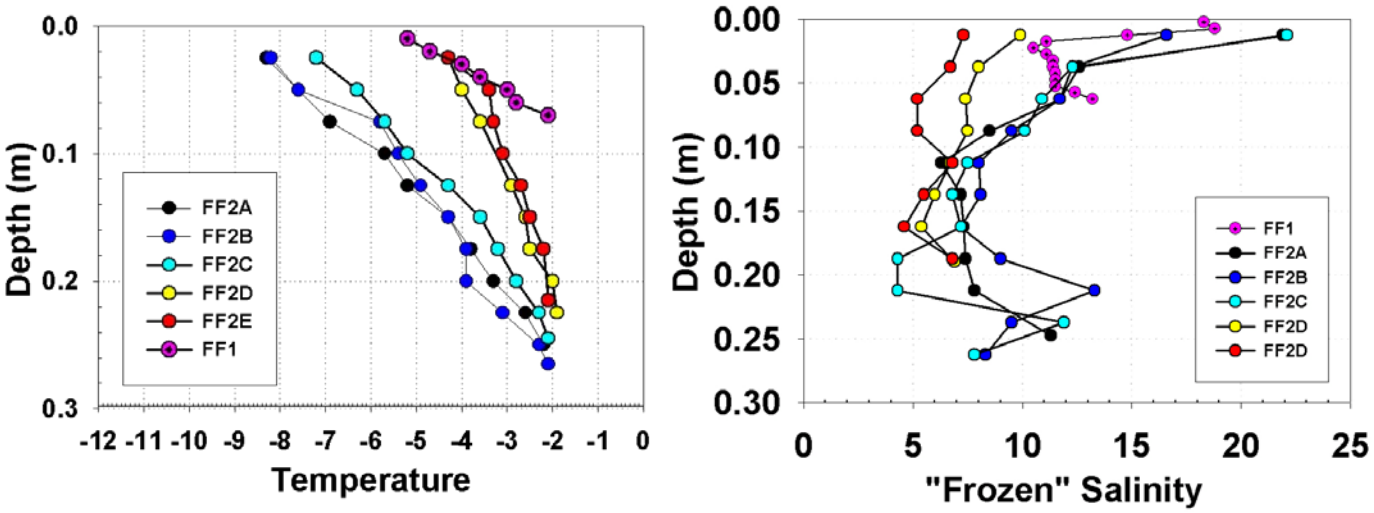

Figure 16 : Temperature and salinity profiles at the Frost Flowers Stations FF1 and FF2 (A to E)

At "Liège", CO_2 fluxes over sea ice ranged from -0.5 to -3 mmol m^{-2} d^{-1}. Temporal evolutions of these fluxes are consistent with the changes in pCO_2 of brines, i.e. enhanced under-saturation leads to the increase of the uptake of CO_2 from the atmosphere. Snow reduces air-ice CO_2 fluxes by 15 to 45 %. This is likely related to the snow structure. Indeed we regularly observed the formation of solid snow layer and ice lenses that impede gas transfers. Further analysis of snow structure and temperature will be conducted to further investigate the effect of snow on air-ice CO_2 fluxes.
At "Bruxelles" site, it is worth noting that the evolution of air-ice CO_2 fluxes is less clear. The magnitude of fluxes is generally lower than in Liège. This is partly due to a lower pCO_2 gradient at the air-ice atmosphere. Also, we observed several striking features that will require further investigations. For example, at three stations the magnitude of CO_2 fluxes over snow was higher than over the ice.

The Frost Flowers Stations

In the early stages of our stay at Station Belgica, while we entered the cooling phase, a large portion of the open waters was covered with new ice formation and a generalized development of “frost flowers”. We have therefore initiated a survey of a frost flowers formation site, in the lead close to the ship docking site (day 277). Several blocks of a 7 cm new ice cover were collected in order to obtain a full description of the physico-chemical characteristics of this new ice and how frost flowers formation is initiated. Given the increasing interest in these features, both for paleoclimatic reconstructions in deep ice cores and for potential impacts on atmospheric chemistry, we will study these in detail on our return back in Brussels. As expected, a high-resolution profile (0.5 cm spacing) indicates very high salinities for this young sea ice cover, and a typical C-shaped profile (Figure 15, FF1).
We revisited the site on day 290. The ice thickness was fairly homogeneous for most part of the site (about 27 cm), depleted of snow cover. However, a small section, close to the lead border, was covered with drifted snow, up to 11 cm thick, and showed reduced ice thickness down to about 20 cm. This peculiar setting has allowed us to study the details of the impact of snow cover on the physical, chemical and biological properties of sea ice. Also, comparing the ice thickness evolution in the course of time (including an intermediary measurement between our two visits) will allow us to reconstruct an estimate of the mean oceanic heat flux during the duration of the experiment. This will be of peculiar importance for the interpretation of the Mass Balance Buoys results and the modelling efforts. High-resolution structure, bulk salinity, temperature, nutrients, gas composition and biological measurements have been initiated on five stations located on a transect perpendicular to the lead walls (and will be followed back on return to our home labs). Bell CO_2 fluxes have also been performed at each station. As discussed in further details below, rom the comparison of the contrasted

temperature profiles and measured CO_2 fluxes, we can already ascertain that the experiment provides a) a first “in-situ” demonstration of the impact of the porosity (law of 5) on gas fluxes at the ice-atmosphere interface and b) a first “in situ” demonstration that production of new ice is (as expected) a temporary source of carbon dioxide to the atmosphere. Only one experimental study has demonstrated this process until now.
Structure studies on the thick sections cut on board indicate that, at all ice locations, granular ice exists on top of the columnar ice. However, as one approaches the lead’s walls and snow thickness increases, the relative contribution of granular ice increases, columnar ice being reduced to the bottom 5 cm (as opposed to 18 cm in the further station), with a total thickness only increasing by 7.5 cm.
Air-ice CO_2 fluxes measurements were carried out during the second frost flowers station using the "chamber method". We measured CO_2 fluxes at 5 locations above thin newly formed sea ice (25 cm thickness in average) along a 15 m transect ranging from uncovered area to snow covered area. The increase of temperature of the ice interface along the transect reflects the increase of snow cover.

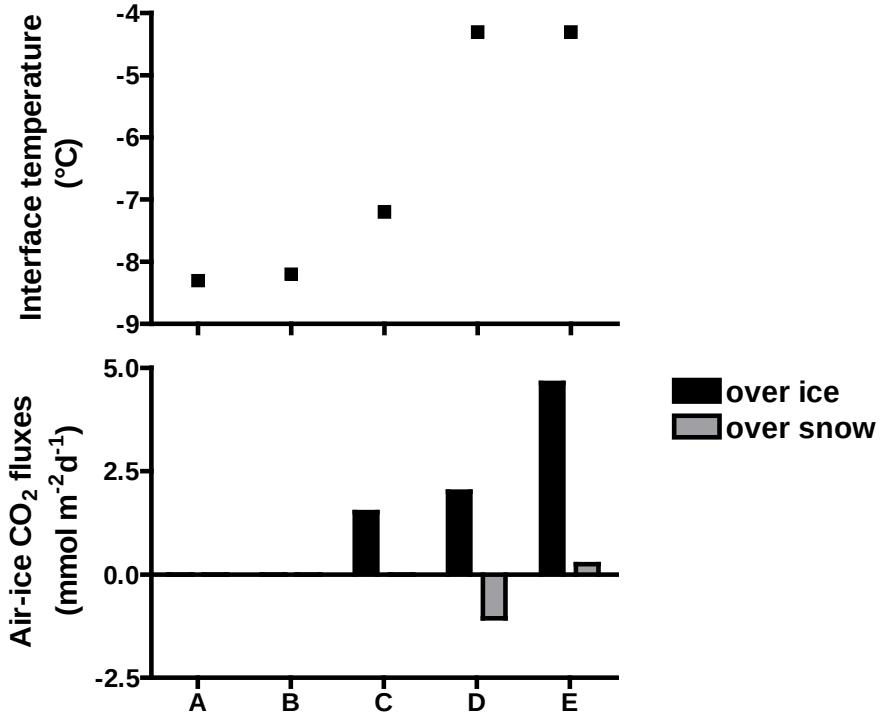

Figure 17: Temperature at the ice interface and CO_2 fluxes over ice and snow (positive fluxes correspond to efflux to the atmosphere) at 5 sites of the second "frost flowers" station**.**

Air-ice CO_2 fluxes were not detected at the two sites where interface temperature was around -8.3 °C. In contrast, at sites where the interface temperature was above -7.2, we observed an increase of air-ice CO_2 fluxes up to 4.6 mmol m^{-2} d^{-1} in parallel to the increase of the interface temperature. Air-ice CO_2 fluxes are partly controlled by the permeability of the air-ice interface that depends of the temperature of the interface. To our best knowledge, very few studies investigated the permeability of gases within sea ice. Golden et al. (1998) showed a rapid drop of permeability for liquid around -5° C depending of the bulk salinity, while Gosink et al. (1976) showed that the ice was permeable to CO_2 at -7°C. Delille et al. (2006) observed that the magnitude of air-ice CO_2 fluxes decreases dramatically around -7°C and did not detect fluxes below -10°C. Here, we observed that the threshold of permeability for CO_2 at this station was between -8.3 and -7.2 °C. Bulk salinity of the ice ranged from 7.3 up to 21.9.

Air-ice CO_2 fluxes are driven by the air-ice pCO_2 gradient. It is generally considered that air pCO_2 is constant compared to pCO_2 of aquatic environments. Hence, while the temperature of the ice is a leading factor in controlling the magnitude of air-ice CO_2 fluxes, pCO_2 of the ice controls both magnitude and direction of the fluxes. There is very scarce evidence of CO_2 degassing from sea ice. It was only observed once over cold ice in Eastern Antarctica (Delille, 2006). However, experimental studies of Nomura et al. (2006) suggested that growing ice can release CO_2 to the atmosphere. This is the first field evidence that young ice is releasing CO_2 to the atmosphere. However, at site D, while the ice can potentially release CO_2 to the atmosphere, flux measurement carried out over the snow exhibits an opposite direction (i.e. towards the ice). Most probable explanation is that a very thin surface community developed at the ice-snow interface and acted to decrease pCO_2 at the skin surface of the ice. This skin layer was likely removed prior to air-ice CO_2 measurement. Indeed, CO_2 fluxes measurements over the ice imply that the snow is removed prior to the measurement. While we paid attention to gently and carefully remove snow, unfortunate removal of such "skin" community can occur. In the same way air-ice CO_2 fluxes is modulated by the structure of snow. While snow can be rather permeable to CO_2 (Takagi et al., 2005), structure of snow, and particularly the formation of solid freshwater ice lenses can prohibit CO_2 transfer. At site E, the structure of snow, as well as potential "skin" communities, appear to hamper air-ice CO_2 fluxes.

Underway pCO_2 and O_2 and CTD casts

The complete description and performance test of the system for pCO_2 measurements was reported by Frankignoulle et al. (2001). Briefly, pCO_2 was measured continuously from the uncontaminated seawater supply of the ship. A non-dispersive infrared gas analyser (IRGA, Li-Cor® LI-6262) was used to measure pCO_2 in air equilibrated with seawater. The IRGA was calibrated daily using three gas standards of 0, 369.4 and 425.8 ppm provided by Air Liquide Belgium®. Seawater flowed into the equilibrator (3 L min^{-1}) from the top, and a closed air loop (3 L min^{-1}) ensures circulation through the equilibrator (from the bottom to the top) and the IRGA. Temperature at the outlet of the equilibrator was monitored using a Li-Cor® temperature sensor. The pCO_2 values were corrected for the temperature difference between *in situ* seawater and water in the equilibrator, using the algorithm proposed by Copin-Montégut (1988; 1989). Oxygen concentration was also continuously measured using an Aanderaa® 3835 oxygen optode.

Underway pCO_2

Underway measurement of pCO_2 and O_2 concentration of surface waters was carried out throughout the cruise (with the notable exception of Chilean waters). Data processing is not completed yet.
The purpose of this underway pCO_2 survey was to further investigate the effect of the interaction of sea ice and underlying water on CO_2 dynamics in both environments. Furthermore, we observed an uptake of atmospheric CO_2 by sea ice cover. However, at the regional scale, this CO_2 uptake is balanced by CO_2 release from the open water area including cracks and leads, as surface waters were oversaturated in CO_2. This counteracting air-sea CO_2 evasion will be assessed from the underway pCO_2 measurement and included in further regional budgets of air-ice-sea CO_2 fluxes.

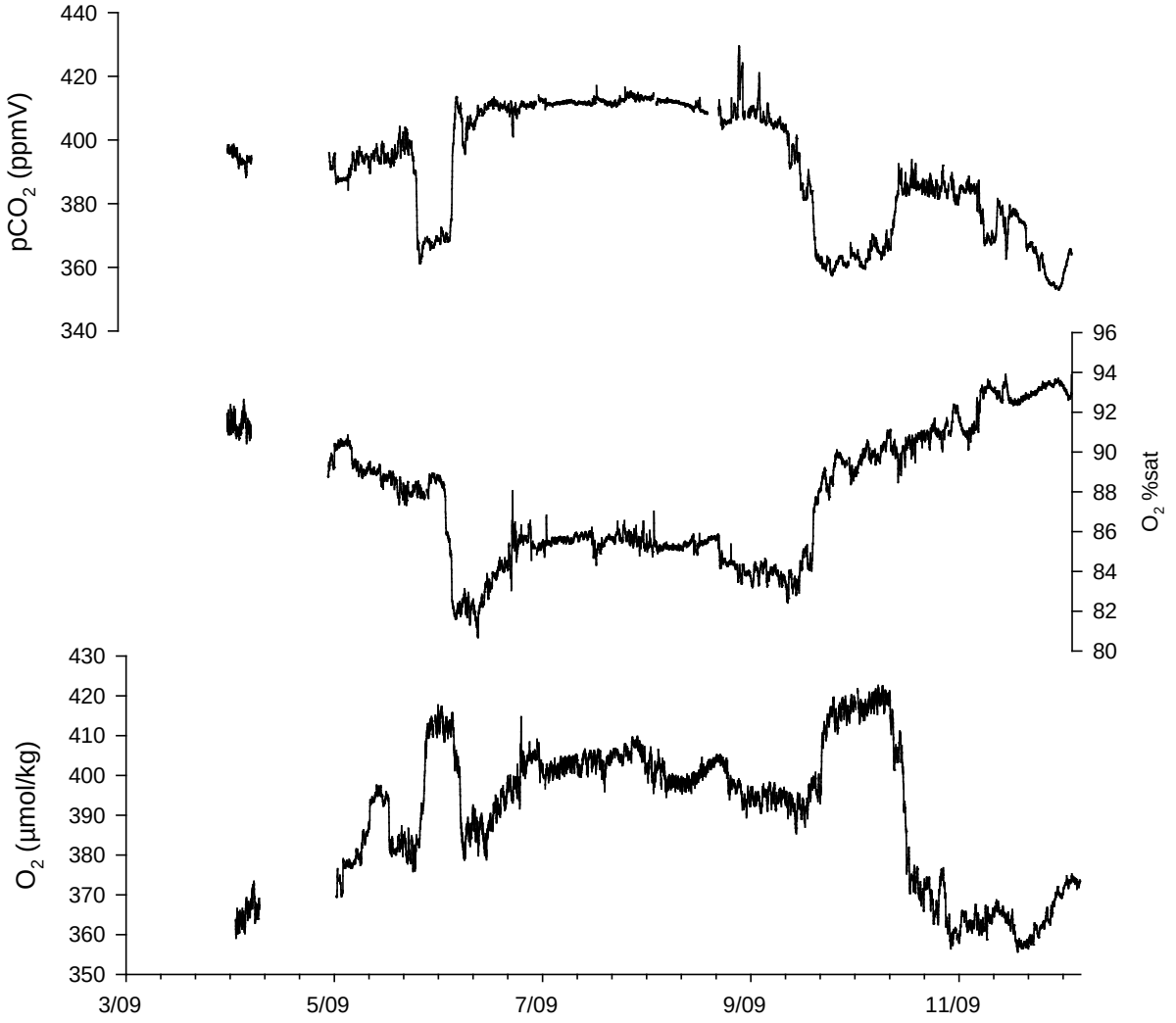

Figure 18: Evolution of pCO_2, oxygen concentration and percentage of oxygen saturation during the first two weeks of the survey (not corrected data).

Finally, underway measurement of pCO_2 was also carried out during this cruise by the group of Pr T. Takahashi of the Lamont-Doherty Earth Observatory (LDEO). The Chemical Oceanography Unit of the University of Liège and the group of Pr T. Takahashi of the Lamont-Doherty Earth Observatory have already contributed to two papers (Rangama et al. 2005; Takahashi et al. submitted) by merging their pCO_2 data set of the Southern Ocean. This survey will serve as an inter-calibration of measurements of both groups.

Anthropogenic CO_2 content of the water column (CTD casts)

We aimed to document anthropogenic CO_2 content of the water column in the Bellingshausen Sea, a poorly sampled area. We therefore collected samples for DIC, TA, pH, nutrients (nitrates, nitrite, ammonium, silicate and phosphate) and oxygen from the surface to the bottom. DIC measurements will be carried out back to the laboratory.

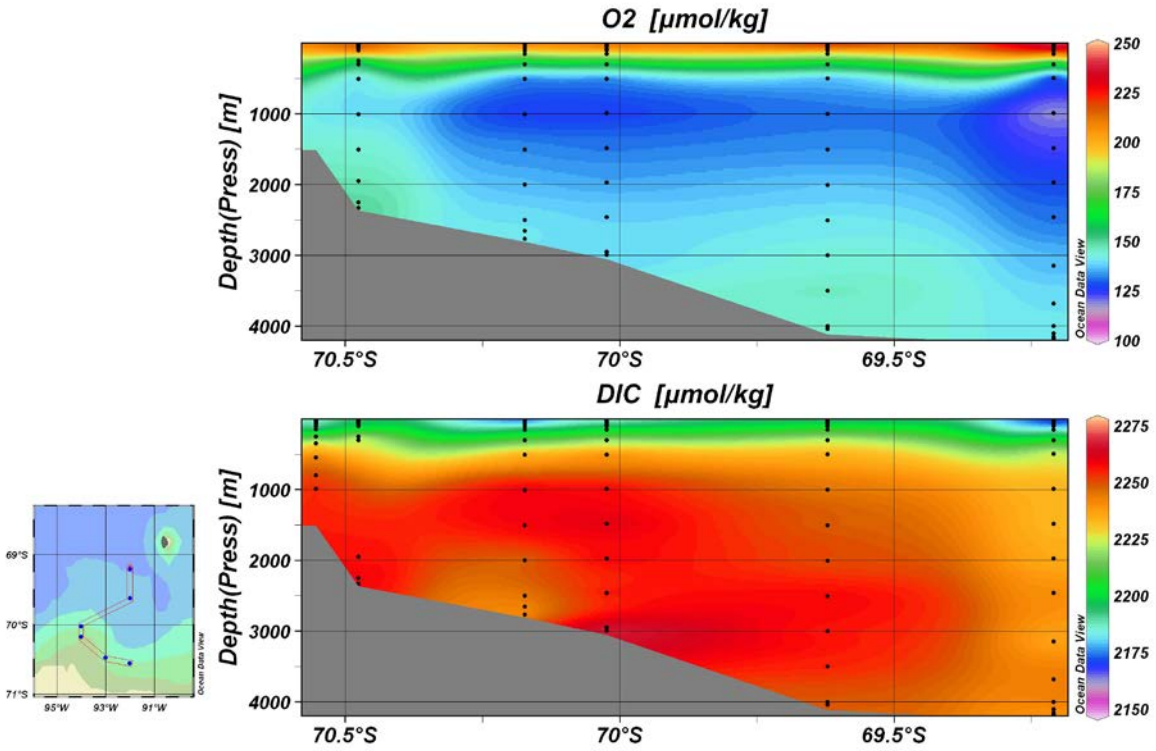

Figure 19: Latitudinal distribution of oxygen concentration and dissolved inorganic carbon computed from pH and total alkalinity during SIMBA cruise (oxygen data require further calibration).

In latitudinal distribution of oxygen and DIC, we observed an increase of oxygen concentration and decrease of DIC towards the bottom. This water is likely corresponding to Antarctic bottom water (AABW). Formation of AABW is generally driven by deep winter convection at the continental shelf and subsequent mixing with circumpolar Current. The significance of the AABW formation to ventilate anthropogenic CO_2 to the ocean interior is still a matter of debate (Sabine et al., 2004; Lo Monaco et al., 2005). As pointed out by Sabine et al. (2004) this uncertainty is due to the lack of data in the area. We will contribute to bridge the gap in the Bellingshausen Sea.

Table 4. List of cast and parameters analysed for anthropogenic carbon determination

cast number	date	Longitude	latitude	maximal depth (db)	number of depth	DIC	TA	pH	O2	Nutrients
1	25/09/2007	-70.256	-90.008	501	11	X	X	X		
2	26/09/2007	-70.417	-90.014	551	16	X	X	X		
3	27/09/2007	-70.625	-90.010	502	13	X	X	X		
4	29/09/2007	-70.553	-92.018	999	14	X	X	X		
5	30/09/1930	-70.476	-93.008	2286	16	X	X	X	X	X
6	4/10/2007	-70.173	-94.014	2810	16	X	X	X	X	X
41	15/10/2007	-69.622	-92.003	4117	18	X	X	X	X	X
67	24/10/2007	-70.024	-94.013	3045	16	X	X	X	X	X
69	25/10/2007	-69.210	-92.003	4279	22	X	X	X	X	X

In addition, Keith Johnson (Institute of Ocean Science – Canada) has also collected samples for DIC (analysed with a "SOMMA" system) and pH (spectrophotometric determination). This will allow to test the second prototype of "AIR-DIC" DIC analyser from Marianda®. The

Chemical Oceanography Unit is presently involved in development and testing of this device prior to marketing phase.

Trace Metal casts

Water column samples were collected from two sampling systems, either a 12 General Oceanics GoFlo bottle epoxy-coated rosette deployed from a 1000m Kevlar co-ax cable and equipped with a Seabird CTD package, oxygen sensor, fluorimeter and transmissiometer ('TMC' in table 5); or a regular 24 General Oceanics Niskin bottle epoxy-coated rosette deployed from a clean stainless steel cable with a similar sensor package ('CTD' in table 5).

Table 5. List of cast and parameters analysed for anthropogenic carbon determination

Hydrocast	Site	Date	Julian day	Lat S	Long W	[Fe]	δ^{56}Fe	Remarks
CTD-002	Underway ice station 2	26/9/2007	269	-70.418	-90.548	x		Niskin 5-550m, 15 depths, seafloor 2350m
TMC-002	Process Station	29/920/07	272	-70.543	-93.002	x		GoFlo 10-1000m, 12 depths, seafloor 1683m
CTD-005	Process Station	30/9/2007	273	-70.478	-93.571	x		Niskin 50-2325m, 10 depths, seafloor 2330m
CTD-006	Process Station	10/04/2007	277	-70.176	-94.512	x		Niskin 1000-2780m, 6 depths, seafloor 2785m
TMC-003	Process Station	10/04/2007	277	-70.174	-94.487	x		GoFlo 10-1000m, 12 depths, seafloor 2792m
CTD-053	Wake ice berg	19/10/07	292	-69.868	-93.130	x		Niskin 10-500m, 12 depths, seafloor 3642m
CTD-067	Process Station	24/10/07	297	-70.027	-94.513	x	x	Niskin 2000m, 3000m, 3044m, seafloor 3052m
TMC-004	Process Station	24/10/07	297	-70.011	-94.668	x	x	GoFlo 50m, 150m, 250m, 1000m, seafloor 2930m
TMC-005	Peter I Island	26/10/07	299	-68.711	-90.803	x		GoFlo 10-1005m, 11 depths, seafloor 1010m

The internal springs of the Niskins were plastic coated. It was recently demonstrated that GoFlo on Kevlar, GoFlo on rosette, or Niskin on rosette yielded the same Fe concentrations in the Pacific sector of the Antarctic Circumpolar Current (Measures and Vink, 2001). GoFLo's from the TMC were taken off the rosette right upon return on board and sub-sampled (1L Nalgene polyethylene bottles) inside the class 100 clean van. CTD Niskins were

sub-sampled at the rosette. Sample filtrations were immediately carried out after sub-sampling. Samples of 250 mL were collected for TD-Fe (unfiltered) and DFe (filtered).
CTD-002 (duplicate bottles closed at several depths) and TMC-002/CTD-005 (overlapping depths) will provide information on cleanliness of Niskins and comparability of both sampling systems. TMC-002/CTD-005, TMC-003/CTD-006 (both western Bellingshausen Sea) and TMC-005 (shelf of Peter I Island) will provide complete surface to seafloor profiles for iron concentrations. CTD-053 was a shallow hydrocast to study the possible input of iron from melting ice and turbulent mixing in the wake of a ~35m high, ~200m wide and ~200m deep iceberg that came to ~500m from the Ice Station Belgica.
Finally, large volume samples (20L) for iron isotopic measurements of dissolved and particulate Fe were collected at seven depths from casts TMC-004/CTD-067, by closing 2 to3 bottles at the selected depths. Samples were processed as described above.

Radiative Balance

This topic has been described in Martin Vancopenolle report

Meteorological Buoy Deployment

We have deployed our first Belgian metocean buoy on the 28th October 2007 at 18:30 GMT and 70°01.688 S / 94°00.094 E on a flat topped bergy bit entrapped in a large floe of sea ice. This buoy will relay position, temperature and pressure for 1 to 2 years via the ARGOS system, provides it survives that long.

References

Copin-Montégut, C., 1988. A new formula for the effect of temperature on the partial pressure of carbon dioxide in seawater. Marine Chemistry 25(1), 29-37 doi:10.1016/0304-4203(88)90012-6.

Copin-Montégut, C., 1989. A new formula for the effect of temperature on the partial pressure of carbon dioxide in seawater, Corrigendum. Marine Chemistry 27(1-2), 143-144 doi:10.1016/0304-4203(89)90034-0.

Delille, B., 2006. Inorganic carbon dynamics and air-ice-sea CO_2 fluxes in the open and coastal waters of the Southern Ocean, University of Liège.

Delille, B., Jourdain, B., Borges, A., Tison, J.-L., Delille, D., 2007. Biogas (CO_2, O_2 , dimethylsulfide) dynamics in Spring Antarctic fast ice. Limnology and Oceanography 52(4), 1367-1379.

Dickson, A.G., Millero, F.J., 1987. A comparison of the equilibrium constants for the dissociation of carbonic acid in seawater media. Deep-Sea Research Part I 34, 1733-1743.

DOE, 1994. Handbook of methods for the anlysis of the various parameters of the carbon dioxide system in sea water.

Frankignoulle, M., 1988. Field measurements of air-sea CO_2 exchange. Limnology and Oceanography 33, 313-322.

Frankignoulle, M., Borges, A.V., Biondo, R., 2001. A new design of equilibrator to monitor carbon dioxide in highly dynamic and turbid environments. Water Research 35(5), 1344-1347.

Gleitz, M., v.d.Loeff, M.R., Thomas, D.N., Dieckmann, G.S., Millero, F.J., 1995. Comparison of summer and winter in organic carbon, oxygen and nutrient concentrations in Antarctic sea ice brine. Marine Chemistry 51(2), 81-91.

Golden, K.M., Ackley, S.F., Lytle, V.I., 1998. The percolation phase transition in sea ice. Science 282(5397), 2238-2241.

Gosink, T.A., Pearson, J.G., Kelley, J.J., 1976. Gas movement through sea ice. Nature 263(2), 41-42.

Lo Monaco, C., Goyet, C., Metzl, N., Poisson, A., Touratier, F., 2005. Distribution and Inventory of Anthropogenic CO_2 in the Southern Ocean: Comparison of three Data-based Methods. Journal of Geophysical Research 110(C09S02), doi:10.1029/2004JC002571.

Mehrbach, C., Culberson, C.H., Hawley, J.E., Pytkowicz, R.M., 1973. Measurements of the apparent dissociation constants of carbonic acid in seawater at atmospheric pressure. Limnology and Oceanography 18, 897-907.

Nomura, D., Yoshikawa-Inoue, H., Toyota, T., 2006. The effect of sea-ice growth on air–sea CO_2 flux in a tank experiment. Tellus B, doi: 10.1111/j.1600-0889.2006.00204.x.

Papadimitriou, S., Kennedy, H., Kattner, G., Dieckmann, G.S., Thomas, D.N., 2004. Experimental evidence for carbonate precipitation and CO2 degassing during sea ice formation. Geochimica et Cosmochimica Acta 68(8), 1749-1761.

Rangama, Y., Boutin, J., Etcheto, J., Merlivat, L., Takahashi, T., Delille, B., Frankignoulle, M., Bakker, D.C.E., 2005. Variability of net air-sea CO_2 flux inferred from in situ and satellite measurements in the Southern Ocean south of Tasmania and New Zealand. Journal of Geophysical Research 110(C9), doi:10.1029/2004JC002619.

Sabine, C.L., Feely, R.A., Key, R.M., Lee, K., Bullister, J.L., Wanninkhof, R., Wong, C.S., Wallace, D.W.R., Tilbrook, B., Millero, F.J., Peng, T.-H., Kozyr, A., Ono, T., Rios, A.F., 2004. The oceanic sink for anthropogenic CO_2. Science 305(5682), 367-371.

Semiletov, I., Makshtas, A., Akasofu, S.I., Andreas, E.L., 2004. Atmospheric CO_2 balance: The role of Arctic sea ice. Geophysical Research Letters 31(L05121, doi:10.1029/2003GL017996).

Takagi, K., Nomura, M., Ashiya, D., Takahashi, H., Sasa, K., Fujinuma, Y., Shibata, H., Akibayashi, Y., Koike, T., 2005. Dynamic carbon dioxide exchange through snowpack by wind-driven mass transfer in a conifer-broadleaf mixed forest in northernmost Japan. Global Biogeochemical Cycles 19(2).

Tison, J.-L., Haas, C., Gowing, M.M., Sleewaegen, S., Bernard, A., 2002. Tank study of physico-chemical controls on gas content and composition during growth of young sea ice. Journal of Glaciology 48(161), 177-191.

Zemmelink, H.J., Delille, B., Tison, J.-L., Hintsa, E.J., Houghton, L., Dacey, J.W.H., 2006. CO_2 deposition over the multiyear ice of the western Weddell Sea. Geophysical Research Letters 33(L13606), doi:10.1029/2006GL026320.